Temperature and Precipitation Projections in the Edwards Aquifer Region

Prepared for:

Edwards Aquifer Authority
900 E. Quincy
San Antonio, TX 78215
Contact: Chad Furl
210-222-2204 ext 149

Prepared by:

ICF
15102 Jones Maltsberger Road
Suite 101B
San Antonio, TX 78247
Contact: Lucas Bare
505-310-3427

July 2024

ICF. 2024. *Temperature and Precipitation Projections in the Edwards Aquifer Region*. Revision A.2. July. (ICF 04503.0.001) San Antonio, TX. Prepared for Edwards Aquifer Authority, San Antonio, TX.

Contents

Tables and Figures

Acronyms and Abbreviations

Abbreviation	Definition
CMIP	Coupled Model Intercomparison Project
EAA	Edwards Aquifer Authority
EAHCP	Edwards Aquifer Habitat Conservation Plan
GCMs	Global Climate Models
IPCC	Intergovernmental Panel on Climate Change
ITP	Incidental Take Permit
RCPs	Representative Concentration Pathways
South Central-CASC	South-Central Climate Adaptation Center
SSPs	Shared Socioeconomic Pathways
WCRP	World Climate Research Programme

Chapter 1
Introduction

To inform the planning process for the Edwards Aquifer Habitat Conservation Plan (EAHCP) Incidental Take Permit (ITP) Renewal, the Edwards Aquifer Authority (EAA) contracted with ICF to analyze historical and projected temperature and precipitation values across the Edwards Aquifer region. The report objectives are as follows:

1. Describe mean temperature and precipitation projections across the Edwards Aquifer region during the 2030–2059 time period.
2. Compare mean spatial and temporal characteristics of the 2030–2059 temperature and precipitation projections with historical values occurring from 1991–2020.
3. Compare minimum precipitation projections during 2021–2060 to measured minimum precipitation values during prolonged periods of historic precipitation drought across the Edwards Aquifer region (1981–2020) and at the San Antonio International Airport weather station (1947–present), which includes the drought of record[i].

Analyzing historical and projected temperature and precipitation values will help EAA understand future surface water and groundwater conditions and assess how spring flow may change under a range of potential climate futures based on multiple climate models (i.e., using a climate ensemble) and greenhouse gas trajectories (i.e., emissions scenarios). Understanding how spring flow may change is necessary for considering how future climate conditions may affect the Covered Species habitat throughout the proposed 30-year permit term.

EAA provided future model and emissions scenario projections of temperature and precipitation for the Edwards Aquifer region. ICF used the climate projections to identify and evaluate the seasonality, timing, and geography of future changes in climate, including projected precipitation changes during noteworthy historical drought lengths. This is an important early step in the modeling workflow of the project. The temperature and precipitation projections will ultimately inform modeled future recharge for the Edwards Aquifer, which will then be used to model projected spring flow. Projected spring flow will eventually be used to evaluate potential impacts on Covered Species as part of the ITP Renewal process.

This report is organized as follows:

- Chapter 2, *Data and Methods*, identifies the Edwards Aquifer region, historical weather data, and future model projections used in the analysis.
- Chapter 3, *Temperature and Precipitation*, discusses historical and projected temperature and precipitation levels.
- Chapter 4, *Drought*, includes discussion of future drought projections.
- Chapter 5, *Discussion*, summarizes findings from the analysis.

2.1 Edwards Aquifer Region

The Edwards Aquifer region consists of nine surface water basins that drain portions of the Texas Hill Country and provide recharge to the aquifer (Figure 1). The basins include portions of the EAA-delineated Recharge Zone, Contributing Zone, and/or Artesian Zone.

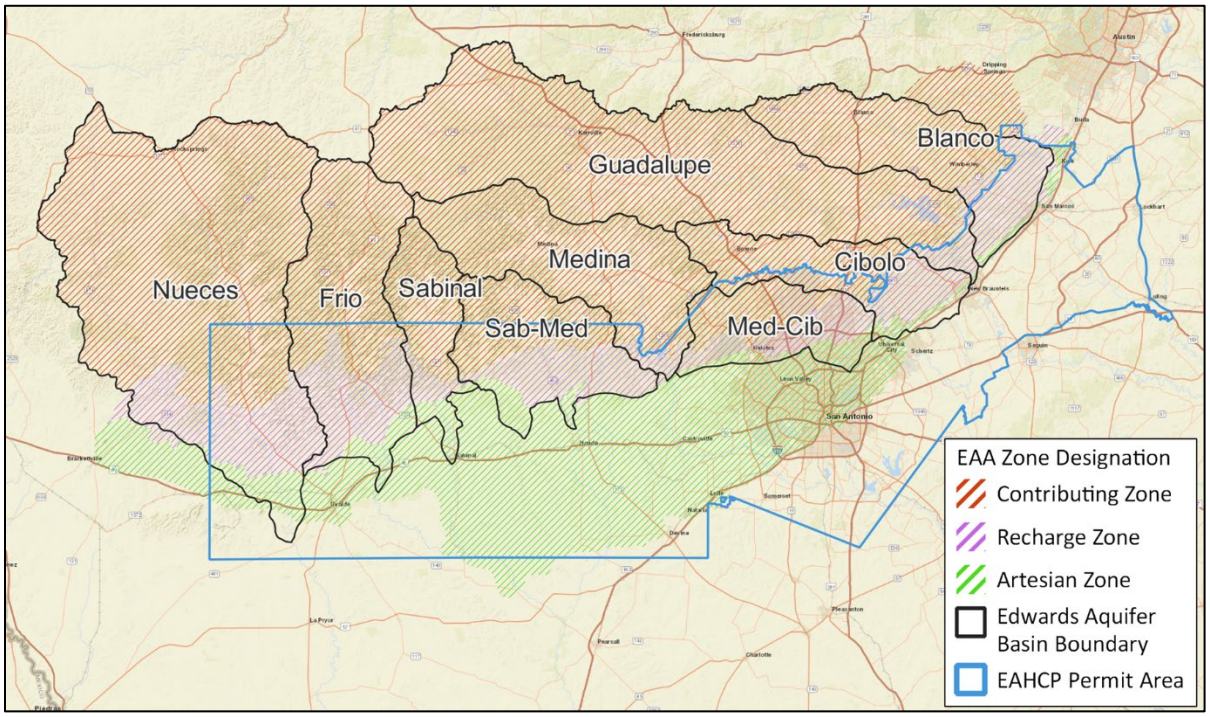

Figure 1. The Edwards Aquifer Region

2.2 Methods

The purpose of this report is to describe near-term projections of future temperature and precipitation and compare with historical climate data to better understand future climate conditions in the Edwards Aquifer region. The analysis considers both average future conditions along with drought conditions.

2.2.1 Description and Comparison of Mean Future Climate

Mean future climate projections from 2030 to 2059 were described and compared to historical weather averages from 1991 to 2020 to evaluate changes in temperature and precipitation that may occur during the proposed permit term (2028–2058). The analysis identifies and evaluates the seasonality, timing, and geography of mean future changes in climate by directly comparing future

monthly and annual projected changes in precipitation and temperature relative to historical weather observations.

For this analysis, 30-year time horizons are used to analyze and describe the mean temperature and precipitation scenarios to minimize the influence of inter-annual climate variance (e.g., the impact of an El Niño event on temperature anomalies) and capture near-future climate change during the proposed permit term. When evaluating climate projections, a common approach is to compare historical and future periods of similar lengths. To that end, the historical time horizon uses the 30 years in the near past (1991–2020) and the future time horizon is evaluated over 30 years in the near future overlapping with the proposed permit term (2030–2059). These time horizons are used to compare composite precipitation and temperature averages during the future and historical time horizons.

Table 1 presents the time horizons used for historical and future mean temperature and precipitation.

2.2.2 Comparison of Historical Droughts to Future Predicted Drought

Drought projections represent worst-case precipitation drought conditions across the Edwards Aquifer region. In contrast to the mean future temperature and precipitation analysis in Section 2.2.1, the purpose of this analysis is to demonstrate how the lowest (or minimum) precipitation values compare during noteworthy drought lengths for the proposed permit term relative to the historical period. Drought projections use the same future Coupled Model Intercomparison Project (CMIP) Global Climate Model (GCM) data but focus over a longer timeframe (2021–2060) to capture more tail-end extremes from a longer sampling of years.

Two analyses of precipitation drought projections are completed using historical gridded Daymet data and historical point-based weather station data at the San Antonio International Airport. Historical Daymet weather data are evaluated over 1981–2020, and historical San Antonio International Airport weather station data are evaluated over 1947–present. Historical San Antonio International Airport weather station data are evaluated for a longer time period relative to the gridded Daymet data to include the drought of record in the 1950s.

For each precipitation drought analysis, the minimum precipitation totals are calculated for consecutive timeframes of 1, 2, 3, 4, and 7.5 years. The precipitation drought lengths correspond approximately with the length of noteworthy historic precipitation droughts in the region, including the drought of record, and were selected based on the methods described in Başağaoğlu et al. (2023). For the gridded Daymet analysis, the minimum precipitation totals are averaged across the Edwards Aquifer region for each historical and future period. For the point-based San Antonio International Airport analysis, the minimum precipitation totals are calculated at the 1 km x 1 km grid cell location overlapping with the airport weather station location. The ensemble mean and full range of model projections for the future timeframe are compared to historical data for each drought length bin.

Table 1 presents the time horizons used for historical and future minimum precipitation during droughts.

Table 1. Scenario Analysis Time Horizons

Analysis	Label	Interval
Mean Future Temperature and Precipitation	Historical	1991–2020
	Future	2030–2059
Gridded Future Minimum Precipitation Droughts	Historical	1981-2020
	Future	2021–2060
Point-Based Future Minimum Precipitation Droughts	Historical	1947–present
	Future	2021–2060

2.2.3 Historical Weather Data

The historical weather data used in this report were primarily drawn from the publicly available, gridded Daymet dataset (ORNL DAAC 2020; Thornton et al. 2020), which provides long-term, continuous, gridded estimates of daily weather and climatology variables by interpolating and extrapolating ground-based weather station observations through statistical modeling techniques (ORNL DAAC 2020). These datasets are provided on 1 km x 1 km spatial grid and are available from 1980 to present day (Thornton et al. 2020). The relevant weather variables drawn from the Daymet version 4 repository include daily precipitation depth, daily maximum temperature, and daily minimum temperature.

The point-based precipitation drought analysis uses ground-based Daily Global Historical Climatology Network (Menne et al. 2012) precipitation depth from the San Antonio International Airport weather station (Station USW00012921). This point-based precipitation dataset is available from 1947 to present day and accessed through the United States National Climatic Data Center Climate Data Online portal.

2.2.4 Future Climate Projections

The World Climate Research Programme (WCRP) coordinates and facilitates climate research across the world. WCRP's CMIP seeks a better understanding of past, present, and future climate changes arising from natural variability and from changes in radiative forcing. One of the main CMIP goals is to make multi-model output (i.e., ensemble simulation results) available in a standardized format (World Climate Research Programme 2020). CMIP future climate projections are released in phases. The Fifth Phase of the CMIP (CMIP5) was released during 2012–2013. The Sixth Phase of the CMIP (CMIP6) was released during 2019–2022.

The EAA, in collaboration with the South-Central Climate Adaptation Center (South Central-CASC), developed and implemented a customized downscaling model to produce statistically downscaled, projected future daily minimum air temperature, daily maximum air temperature, and daily precipitation depth from CMIP5 and CMIP6 GCMs (Wootten et al. 2023). These projections are downscaled to the 1 km x 1 km spatial resolution of the Daymet dataset.

Given that climate change is a result of changes in global greenhouse gas emissions, different climate projections can be formulated using different greenhouse gas emissions scenarios. To understand potential future climate projections, scientists have developed different emissions scenarios derived from global socioeconomic and greenhouse gas emissions pathways. Representative Concentration Pathways (RCPs) were originally developed for use by the Intergovernmental Panel on Climate Change (IPCC) for use in CMIP5. Different RCP scenarios depict alternative options for how global

greenhouse gas emissions could evolve over the course of this century. The RCP scenarios make assumptions about fossil fuel use, technological evolution, population growth, and other driving factors. Shared Socioeconomic Pathways (SSPs) were developed specifically for use in CMIP6. Like RCPs, SSPs represent a range of future climate change scenarios and development pathways that encompass various trajectories of global greenhouse gas emissions. Unlike RCPs, SSPs were also coupled with assumptions about the level of ambition for mitigating climate change. RCP 4.5 and SSP2-4.5 represent a moderately warmer future and assume significant mitigation of greenhouse gas emissions by mid-century. RCP 8.5 and SSP5-8.5 represent a hotter future where emissions continue largely unabated through the end of the century.

Future climate projections used in the CMIP multi-model outputs utilize RCPs and SSPs as potential future climate trajectories. These efforts also support the IPCC assessment reports that offer comprehensive information on the scientific, technical, and socio-economic knowledge on climate change, future impacts and risks, and different mitigation and adaptation options. The fifth assessment report (AR5) was published in 2014 and the sixth assessment report (AR6) was published in 2021.

As part of this analysis, six CMIP6 GCMs and two emissions scenarios (SSP2-4.5 and SSP5-8.5) were selected as the primary basis for the temperature and precipitation scenarios. Four CMIP5 GCMs and two emissions scenarios (RCP 4.5 and RCP 8.5) were also selected as a secondary, or supplementary, basis for temperature and precipitation projections. The EAA provided the future model and emissions scenario outputs on the Daymet 1 km x 1 km spatial grid for the Edwards Aquifer region. Model-based probabilistic projections are evaluated using the model ensemble averages and individual models, including model percentiles, to characterize a full range of potential climate change outcomes. Table 2 lists the CMIP6 models and emissions scenarios, and Table 3 lists the CMIP5 models and emissions trajectories. Annual time series for the full time period (1991–2059) are provided in Section 3.2.2 to illustrate interannual variability in temperature and precipitation across the Edwards Aquifer region.

Table 2. Future CMIP6 Models and Emissions Trajectories

Model Name	Emissions Trajectories
EC-Earth3	SSP2-4.5, SSP5-8.5
INM-CM4-8	SSP2-4.5, SSP5-8.5
INM-CM5-0	SSP2-4.5, SSP5-8.5
KACE-1-0-G	SSP2-4.5, SSP5-8.5
KIOST-ESM	SSP2-4.5, SSP5-8.5
MPI-ESM1-2-HR	SSP2-4.5, SSP5-8.5

Table 3. Future CMIP5 Models and Emissions Trajectories

Model Name	Emissions Trajectories
CMCC-CM	RCP 4.5, RCP 8.5
HadGEM2-CC	RCP 4.5, RCP 8.5
inmcm4	RCP 4.5, RCP 8.5
MRI-ESM1	RCP 8.5

Chapter 3
Temperature and Precipitation

Future mean temperature and rainfall projections, introduced in Section 2.2.4, are described and analyzed in this section relative to historical conditions. Historical climate data are described in Section 3.1, and Section 3.2 describes and analyzes future temperature and rainfall projections relative to the historical data.

The time series are divided into the time horizons shown in

Table 1. Historical weather data are used for 1991–2020. Future CMIP GCM simulations provided by EAA are used for 2030–2059.

3.1 Historical Climate

3.1.1 Key Takeaways

- Precipitation varies across the Edwards Aquifer region by both geography and season. Historically, the eastern portion of the region has experienced more precipitation than the western portion of the region. There are strong seasonal trends in precipitation as well, with relative peaks in late spring (May) and early fall (September) on average.
- Temperature tends to be greatest in the southern portion of the Edwards Aquifer region and lowest in the northwestern portion. Seasonally, temperatures peak in August.
- Maps of historical precipitation and temperature in the region capture local topography, with higher elevations of the Texas Hill Country experiencing higher precipitation totals and cooler temperatures relative to surrounding valleys.

3.1.2 Results

The 1991–2020 time horizon was used to aggregate daily weather parameters to a historical climate description for the Edwards Aquifer region.

Figure 2 shows mean historical annual precipitation values between 1991 and 2020. As the figure illustrates, the eastern portion of the Edwards Aquifer region experiences more precipitation than the western portion. This leads to a west-to-east, dry-to-wet gradient across the region. This precipitation is most concentrated in the Blanco, Cibolo, Med-Cib, and eastern Guadalupe basins. Nueces, the farthest west basin, is historically dry relative to the other basins in the Edwards Aquifer region. Given the high spatial resolution of the historical values, this map also captures topography across the region, illustrating that higher elevations experience higher precipitation totals that runoff into the lower-elevation rivers and streams in each basin. Lower precipitation totals highlight the locations of valleys surrounded by hills and mountains within each basin.

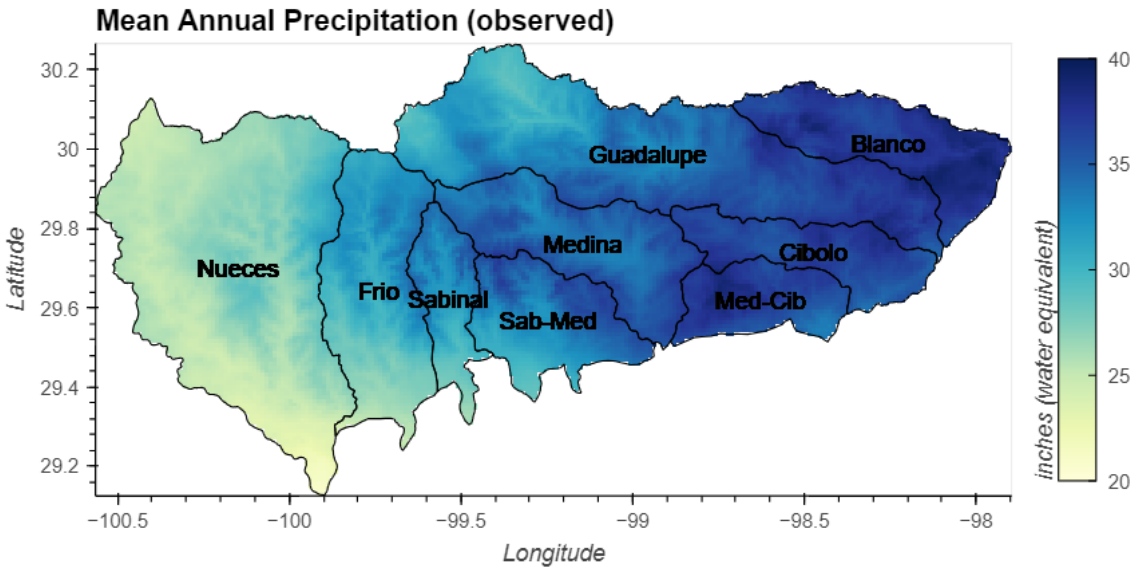

Figure 2. Mean Annual Total Precipitation over the Edwards Aquifer Region (1991–2020) based on Daymet Version 4 Reanalysis

Figure 3 shows mean annual temperature values across the basin between 1991 and 2020. As the figure illustrates, average annual temperatures are generally higher in the southern portion of the Edwards Aquifer region, peaking at 74–75 ˚F in the southern tip of the Nueces basin. The northwestern part of the Guadalupe basin has the lowest average annual temperatures (63–64 ˚F). The historical average annual temperature map also captures topography across the region, with higher elevations experiencing cooler temperatures relative to the lower-elevation valleys in each basin.

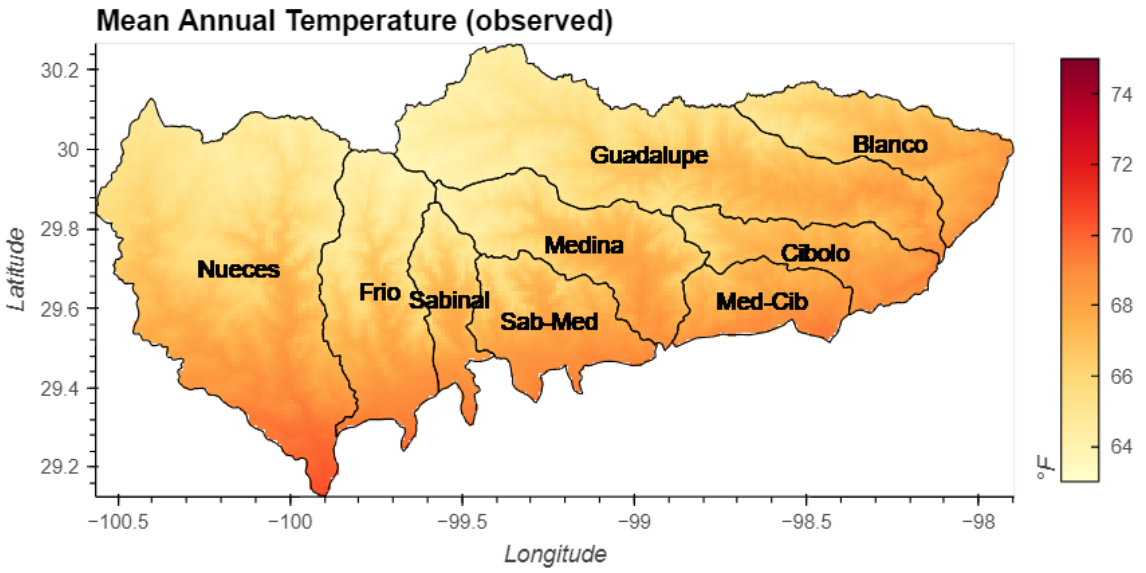

Figure 3. Mean Annual Temperature over the Edwards Aquifer Region (1991–2020) based on Daymet Version 4 Reanalysis

Figure 4 shows monthly mean daily minimum and maximum temperatures averaged across the Edwards Aquifer region between 1991 and 2020. The figure illustrates seasonal variation in temperatures, with temperatures reaching their peak for the year in August and their low for the year in December and January. Daily minimum and maximum temperatures follow similar seasonal trajectories in magnitude throughout the year.

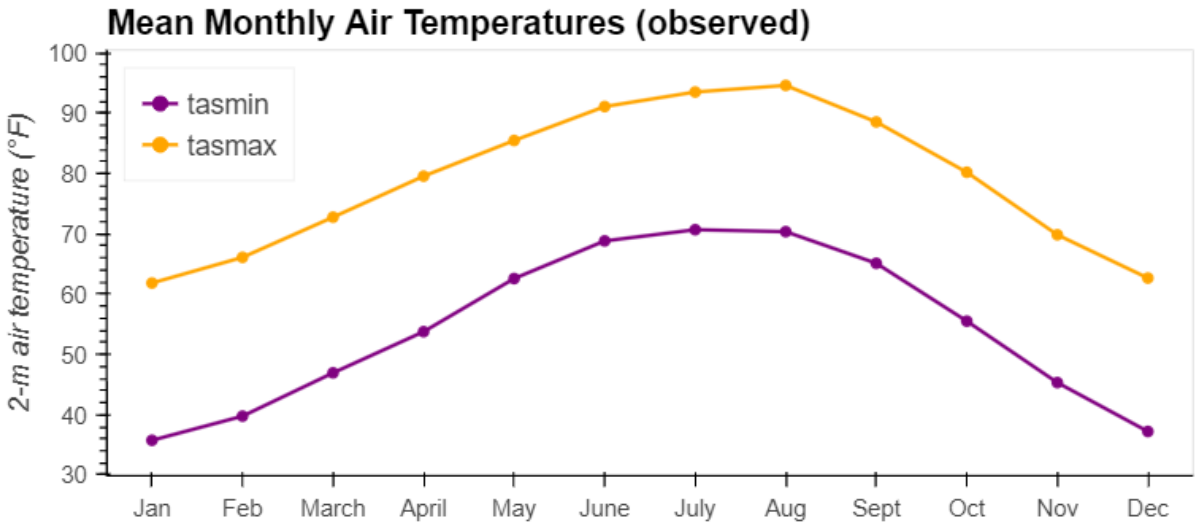

Figure 4. Historical Monthly Mean Daily Minimum/Maximum Temperature (1991–2020) averaged over the Edwards Aquifer Region based on Daymet Version 4 Reanalysis

Figure 5 shows historical monthly precipitation over the Edwards Aquifer region averaged across 1991–2020. May has the highest total precipitation (4.4 inches) while February has the lowest total precipitation (1.6 inches). There is strong seasonal variation in precipitation patterns, with peaks in precipitation in both the spring (May) and the fall (September). This bimodal precipitation

distribution is ubiquitous in central Texas, peaking in May and October separated by a trough with low points in July and August. The historical lower precipitation totals in July and August are important because July and August are also the warmest months with the largest average temperature.

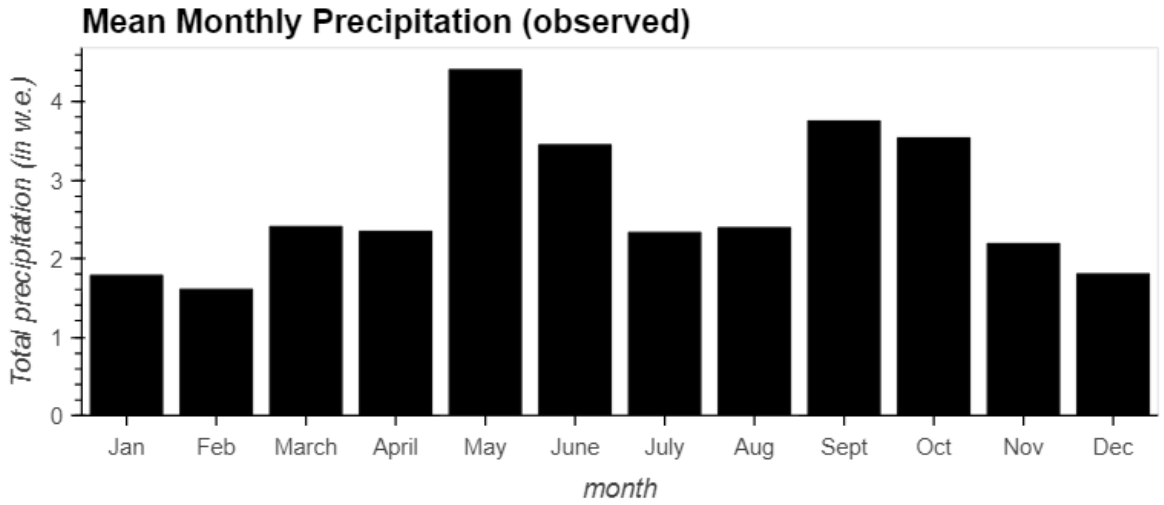

Figure 5. Historical Monthly Precipitation (1991–2020) averaged over the Edwards Aquifer Region based on Daymet Version 4 Reanalysis

3.2 Future Projections

3.2.1 Key Takeaways

- Ensemble mean climate projections indicate minimal change in annual total precipitation depth relative to historical values and changes in seasonal precipitation such that summers are projected to be wetter while there is an attenuation of the springtime peak in precipitation. The greatest rates of precipitation decrease are projected in the western portion of the Edwards Aquifer region.
- There is high model variability in future precipitation projections which indicates a high degree of uncertainty in future precipitation trends across the region.
- Temperatures are projected to increase across the Edwards Aquifer region through 2059. The magnitude and extent of projected change is greater under the higher emissions scenarios, with the greatest rates of warming projected in the western portion of the region.

3.2.2 Results

One future time horizon, 2030–2059, was used to aggregate daily weather parameters to a projected future climate description for the Edwards Aquifer region.

Figure 6 presents projected model-averaged total annual precipitation over the Edwards Aquifer region from 2030 to 2059 under both CMIP5 and CMIP6 model ensembles as well as for two different climate emissions pathways for each ensemble. Under both model ensembles, precipitation

is projected to continue to be greater in the eastern half of the Edwards Aquifer region with the Blanco, western Guadalupe, Cibolo, and Med-Cib basins receiving the most precipitation. Compared to the rest of the basins, the western-most basin, Nueces, will experience lower precipitation totals. In CMIP5 model ensembles, the higher emissions scenario (RCP 8.5) is projected to bring slightly more precipitation as illustrated most clearly in the western-most basin projection. In CMIP6 model ensembles, the higher emissions scenario appears to result in a slightly drier western-most basin.

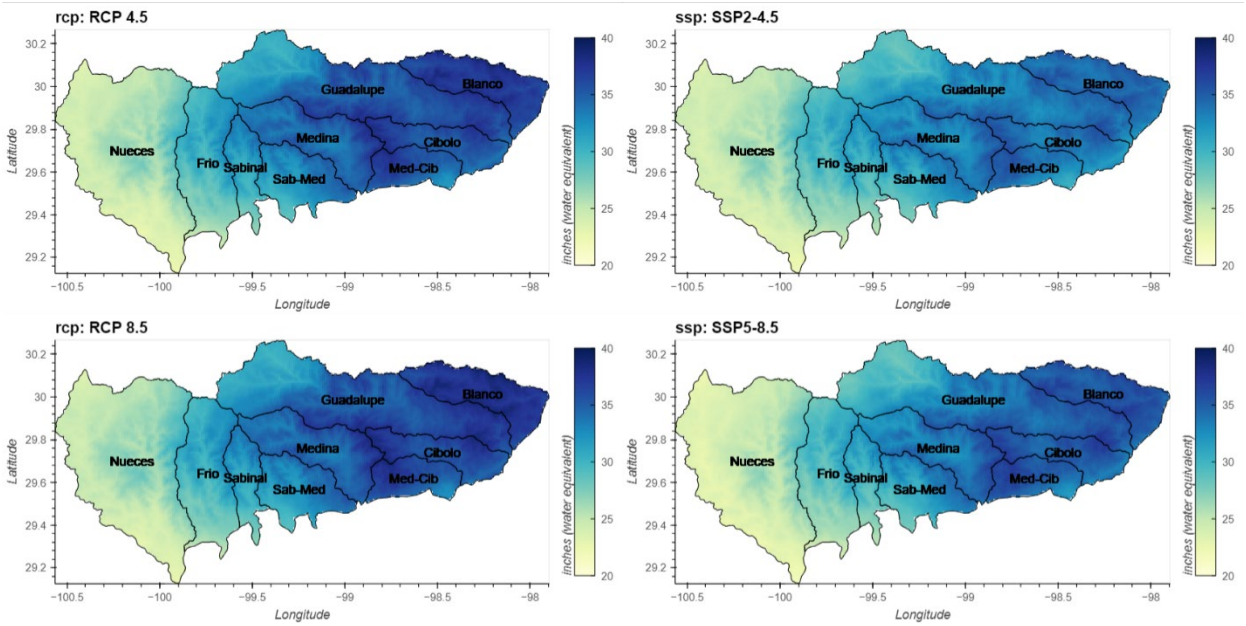

Figure 6. Projected Model-Averaged Total Annual Precipitation over the Edwards Aquifer Region (2030–2059)

The CMIP5 model ensemble is shown on the left and the CMIP6 model ensemble is shown on the right. Two corresponding emissions pathways are presented for each ensemble (top/bottom). Figure represents the ensemble mean for each emissions scenario (RCP/ SSP).

Figure 7 presents the percent change in projected model-averaged total annual precipitation over the Edwards Aquifer region for the period 2030–2059 relative to 1991–2020. Under CMIP5 RCP 4.5 projections, most of the Edwards Aquifer region will experience a decrease in precipitation (i.e., a drying trend), with the greatest drying occurring in the Nueces basin in the western side of the region. However, the southern-most tip of the Nueces basin and the central portion of the Guadalupe basin are projected to experience a slight increase in precipitation. Under CMIP5 RCP 8.5 projections, a less intense drying trend is expected relative to CMIP5 RCP 4.5 projections and more of the region is expected to experience a slight increase in precipitation. Under CMIP6 SSP2-4.5 projections, most of the basin is projected to experience a drying trend except for the southernmost tip of the Nueces basin and the southern border of the Frio basin, both of which may experience slight increases in precipitation. Drying is projected to be most pronounced in the eastern portion of the Edwards Aquifer region. Under CMIP6 SSP5-8.5 projections, the drying trend is projected to be more pronounced in the western portion of the region than under the lower emissions pathway, while projected drying in the eastern portion of the Edwards Aquifer region is less pronounced relative to the SSP2-4.5 emissions scenario.

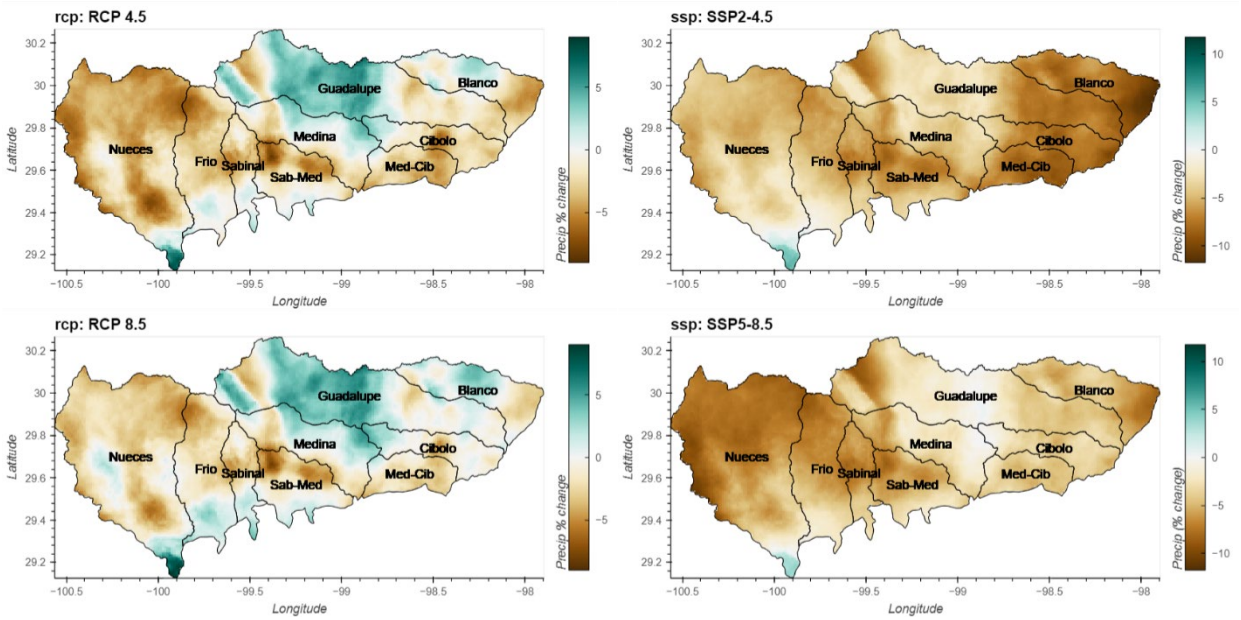

Figure 7. Percent Change in Projected Model-Averaged Total Annual Precipitation (2030–2059) over the Edwards Aquifer Region Relative to the Historical Period (1991–2020)

CMIP5 model ensemble mean results are on the left and CMIP6 ensemble mean results are on the right, with corresponding emissions pathways on the top/bottom. Panels represent the ensemble means for each emissions scenario (RCP/SSP).

Figure 8 shows projected mean annual temperatures over the Edwards Aquifer region between 2030 and 2059 under both CMIP5 and CMIP6 model ensembles and for two different emissions pathways. Under all model ensembles and emissions trajectories, the southern half of the region is projected to experience warmer temperatures.

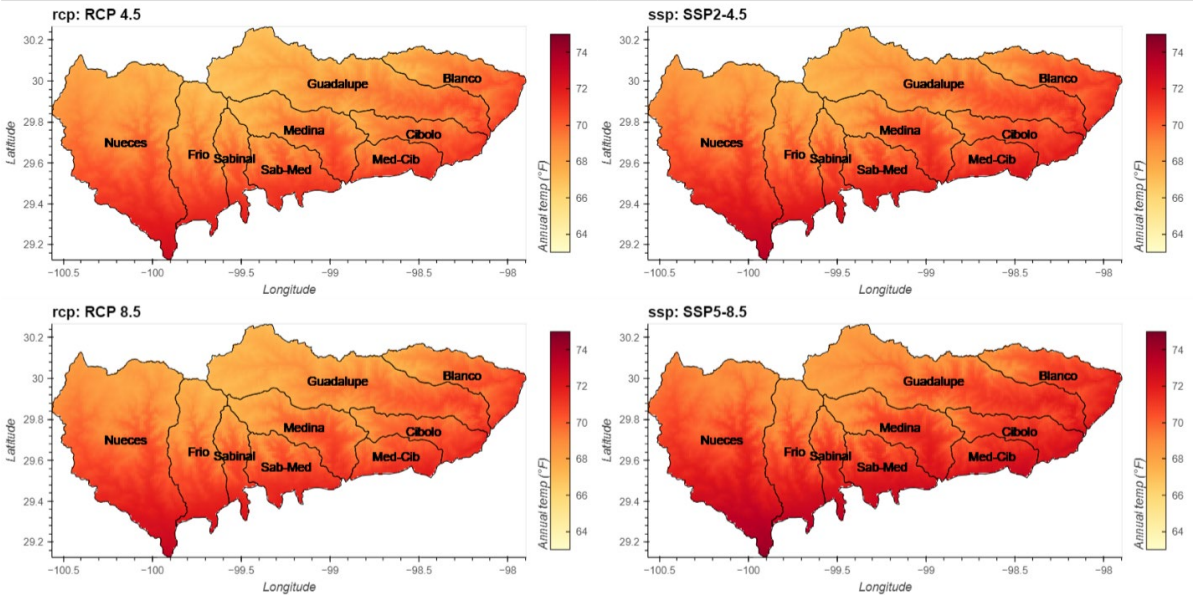

Figure 8. Projected Mean Annual Temperature over the Edwards Aquifer Region (2030–2059)

The CMIP5 model ensemble is on the left and the CMIP6 model ensemble is on the right. Two corresponding emissions pathways are presented for each ensemble (top/bottom). Panels represent the ensemble means for each emissions scenario (RCP/SSP).

Figure 9 illustrates the difference in projected mean annual temperature for the period 2030–2059 relative to 1991–2020 across the Edwards Aquifer region. In the CMIP5 model under RCP 4.5, the difference is most pronounced in the northwestern parts of the region, with the northern part of the Nueces and Frio basins and the western parts of the Medina and Guadalupe basins showing the greatest difference in mean annual temperatures relative to the historical period. Under RCP 8.5, the difference in mean annual temperature is greater across the region with the same trends as historical under RCP 4.5. The CMIP6 projections show greater differences in projected mean temperature across the region relative to the CMIP5 model ensembles. The differences are most pronounced in the northwestern basins and are greater under the high emissions scenario (SSP5-8.5) than the low emission scenario (SSP2-4.5).

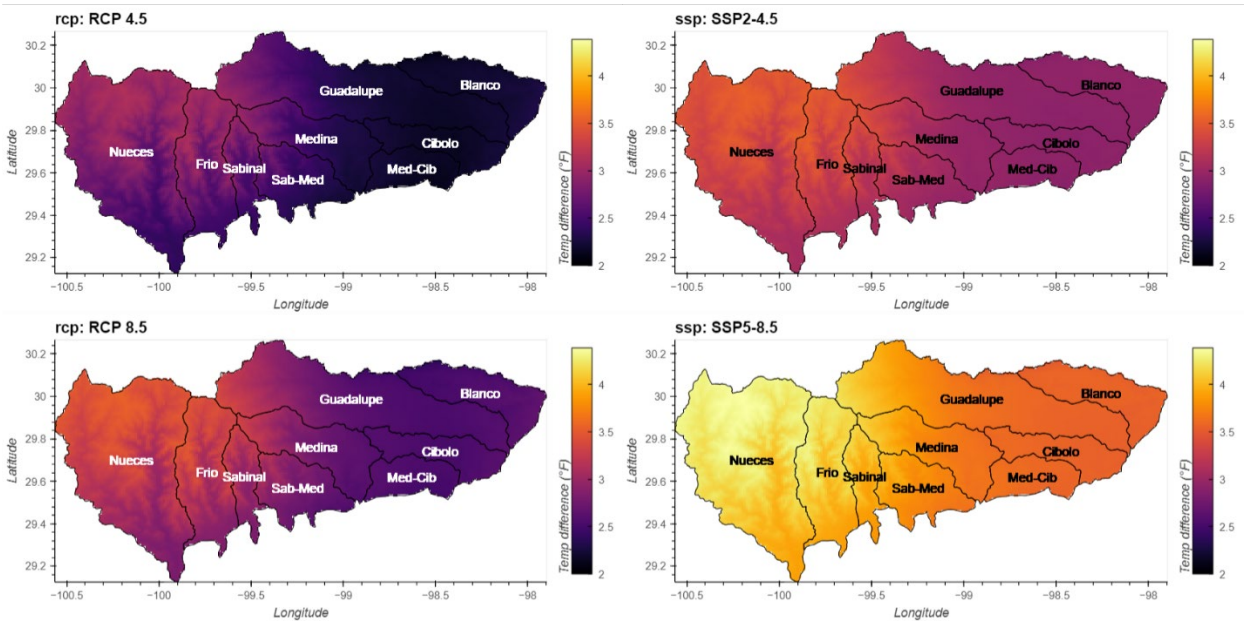

Figure 9. Difference in Projected Mean Annual Temperature (2030–2059) over the Edwards Aquifer Region Relative to the Historical Period (1991–2020)

CMIP5 model ensemble results are on the left, and CMIP6 ensemble results are on the right, with corresponding emissions pathways on the top/bottom. Panels represent the ensemble means for each emissions scenario (RCP/SSP).

As Figure 10 illustrates, temperatures are projected to increase through 2059 relative to historical temperatures. Trends vary across models, with some models projecting greater warming than others. All models, however, do suggest some degree of warming, and there is little difference between the model ensemble means for each emissions trajectory until after 2050 at which point warming is projected to be greater under a higher emissions scenario (RCP 8.5 or SSP2-4.5).

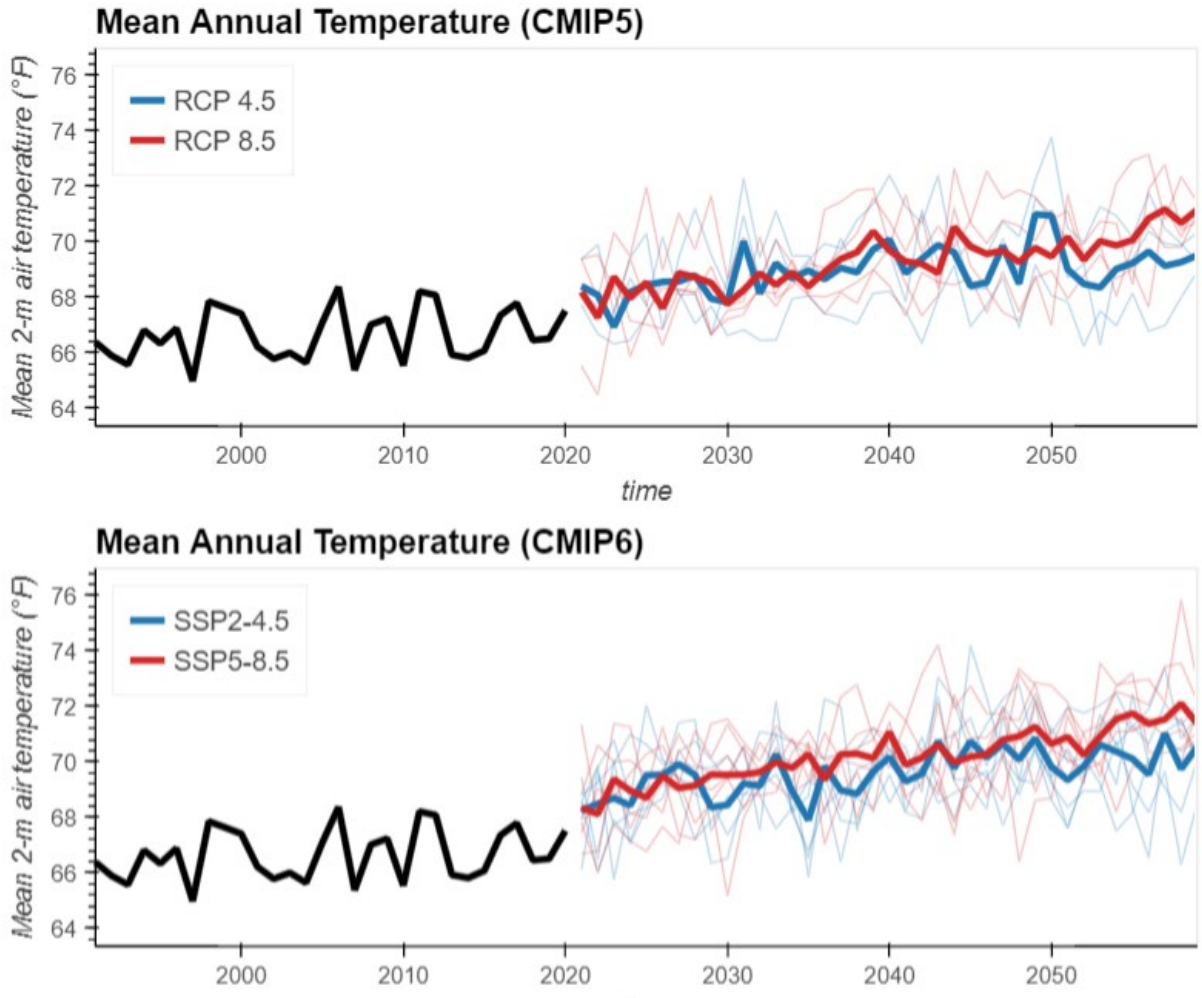

Figure 10. Historical and Projected Annual Average Temperatures

The CMIP5 model ensemble is on the top, and the CMIP6 model ensemble is on the bottom. Two corresponding emissions pathways are included for each model ensemble (blue and red lines). Bold lines denote model ensemble means, while thin lines denote individual model realizations within the ensemble.

As Figure 11 illustrates, models vary in projecting future precipitation through 2060. The high degree of variability between model projections leads to a static, or limited, ensemble mean trend in precipitation projections through 2059. In addition, there is high interannual variability in precipitation which drives anomalously high and low precipitation years in some models.

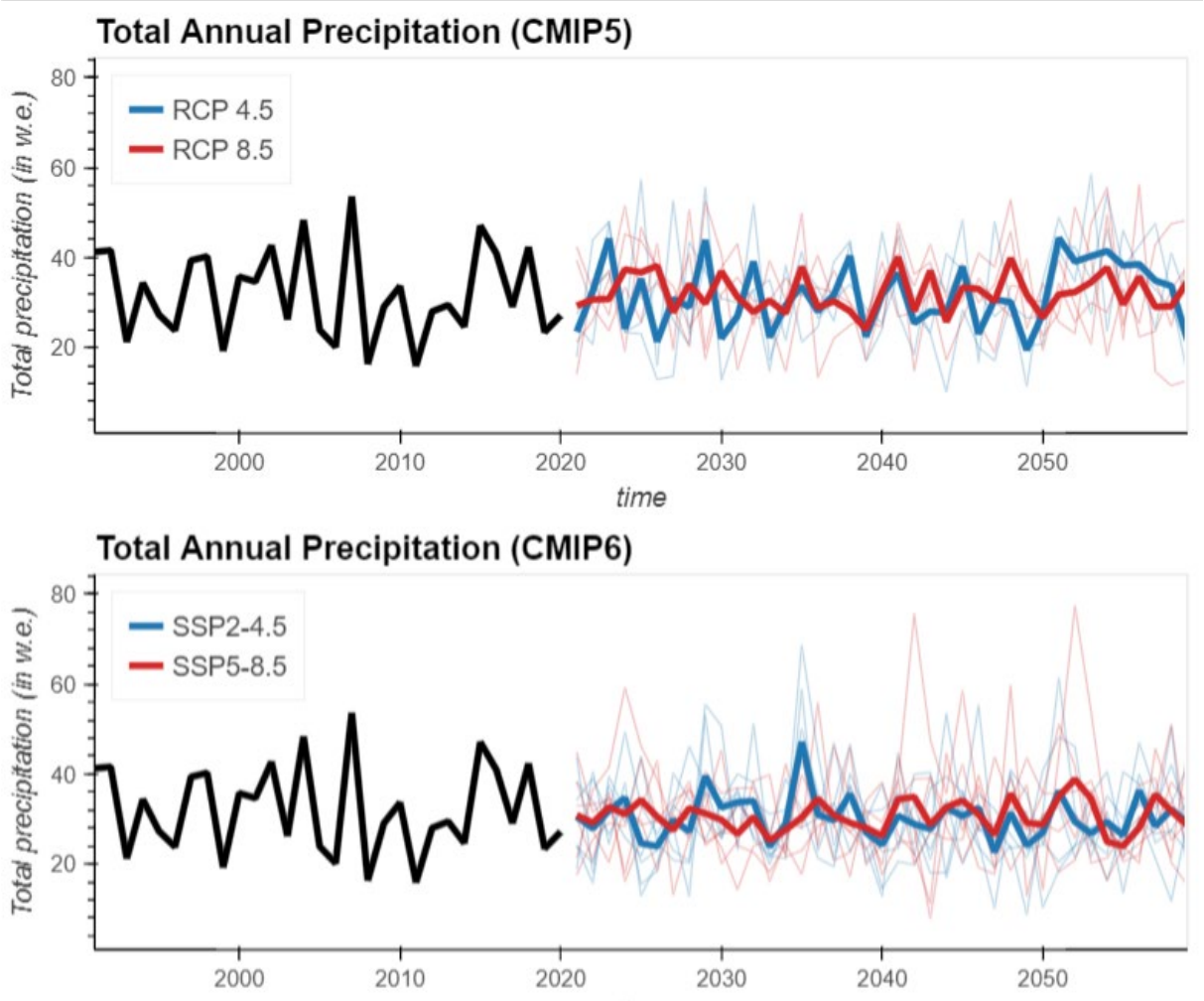

Figure 11. Historical and Projected Total Annual Precipitation

The CMIP5 model ensemble is on the top, and the CMIP6 model ensemble is on the bottom. Two corresponding emissions pathways are included for each model ensemble (blue and red lines). Bold lines denote model ensemble means, while thin lines denote individual model realizations within the ensemble.

Figure 12 illustrates seasonal and monthly variation in projections of temperatures for 2030–2059 for CMIP5 and CMIP6 model ensembles using violin plots. Across models, temperatures peak in June, July, and August and reach their yearly lows in December and January. Temperatures are projected to be higher between 2030 and 2059 relative to historical temperature for both CMIP5 and CMIP6 model ensembles and for both emissions pathways. Projections under the low emissions scenario suggest slightly smaller increases in temperature relative to the higher emissions scenario although the differences are minimal given the near-term and mid-century timeframe. Greater differences between emissions trajectories would be expected later in the century. Equivalent monthly temperature plots for the nine basins within the Edwards Aquifer region are provided in Appendix A.

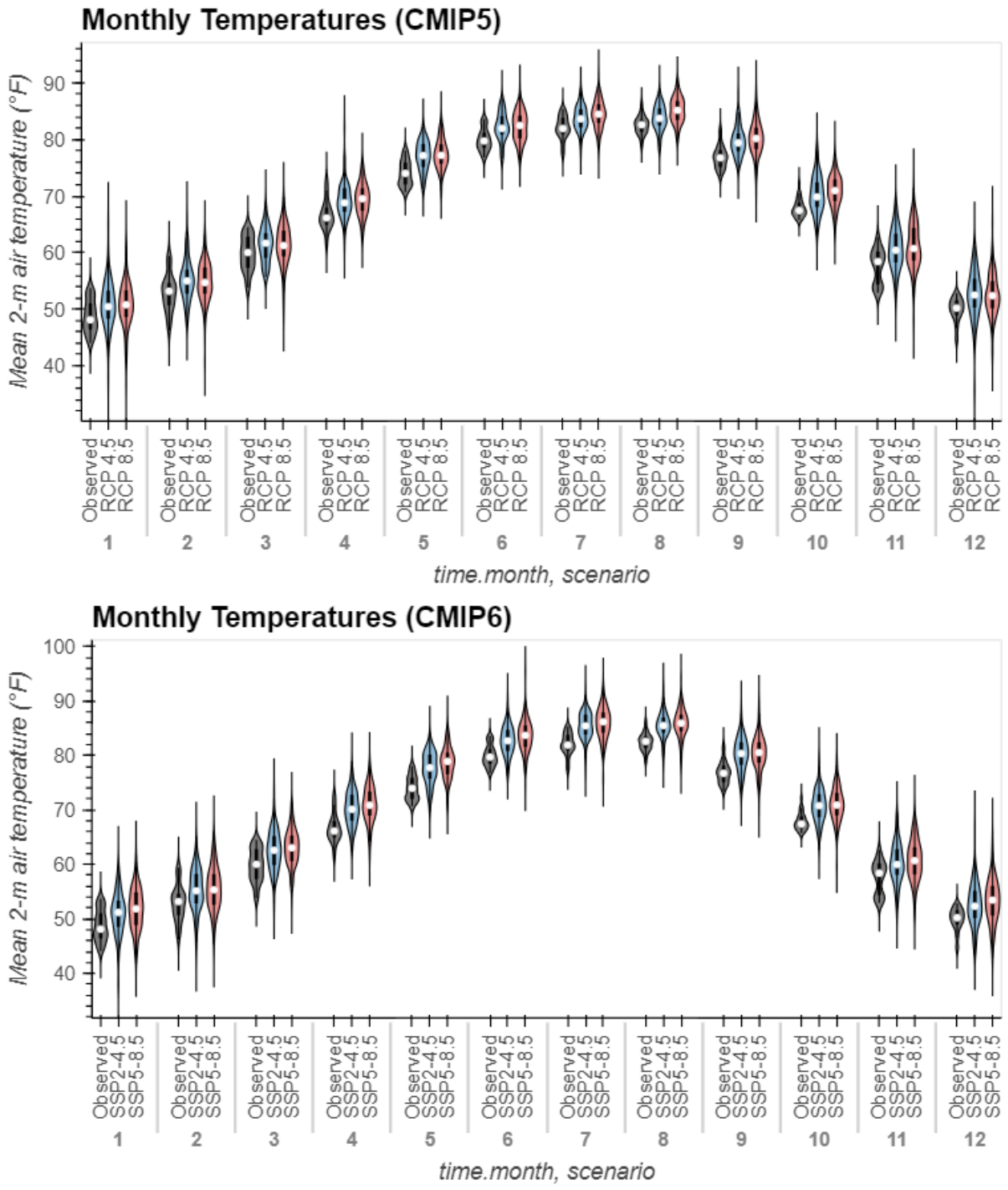

Figure 12. Violin Plot Distributions of Average Basin-Wide Monthly Temperatures (2030–2059)

CMIP5 model ensemble is on the top, and CMIP6 model ensemble is shown on the bottom, with two corresponding emissions trajectories. The historical distributions in monthly temperatures (1991–2020) are denoted in black in both subfigures. White dots denote ensemble mean values while black bars represent the 25th–75th interquartile range. Horizontal widths of violin plots represent the density of values (wider = more models with monthly values).

Figure 13 illustrates projected model-averaged monthly total precipitation across the Edwards Aquifer region during 2030–2059 and 1991–2020. Historically, precipitation has been variable throughout the year, and it is projected to stay variable in the future. While there appears to be a slight trend toward drier conditions relative to historical conditions, there is high variability in future precipitation trends. Some months show increased precipitation while other months show decreased precipitation relative to historical values. Generally, there appears to be a trend toward wetter summers and an attenuation of the spring (May) peak in precipitation under future projections. Equivalent monthly precipitation plots for the nine basins within the Edwards Aquifer region are provided in Appendix A.

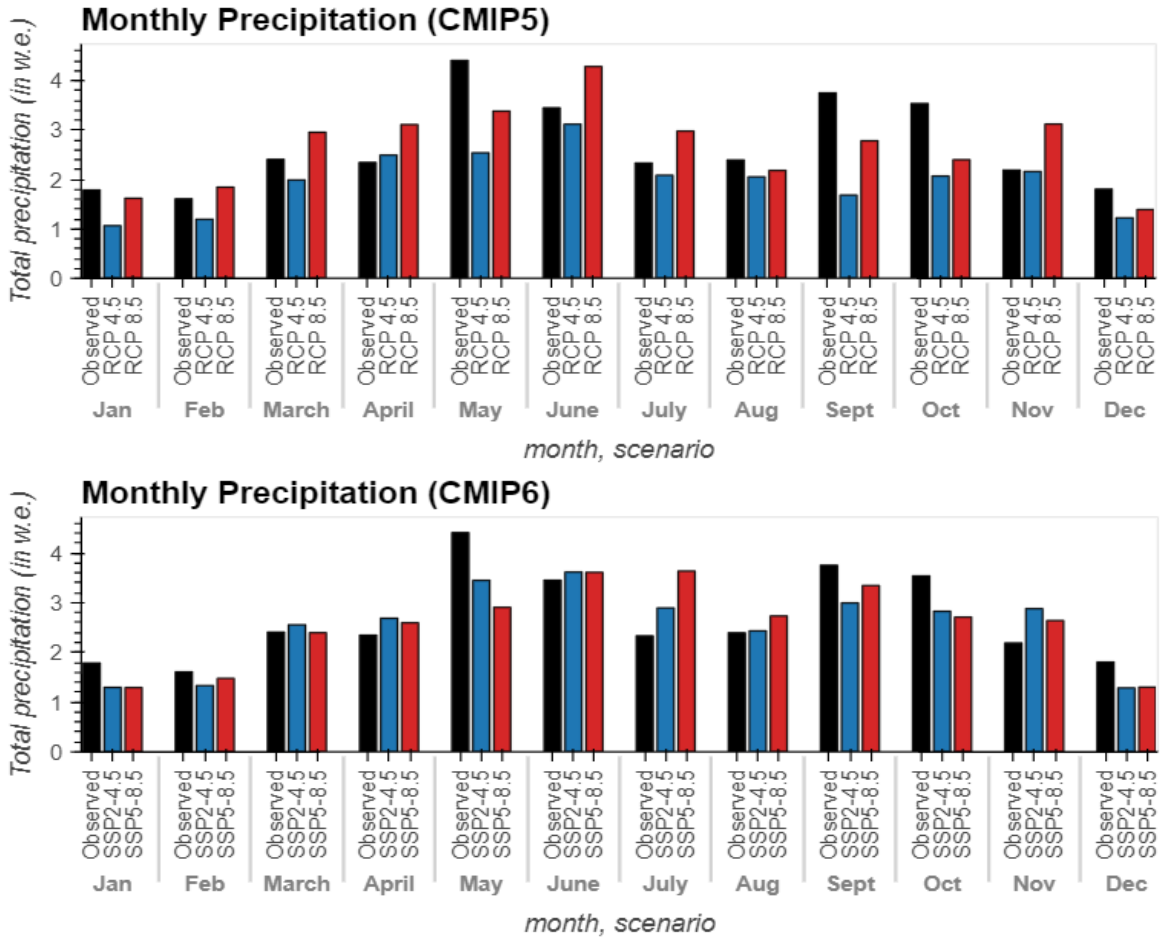

Figure 13. Model-Averaged Monthly Total Precipitation (2030–2059) averaged over the Edwards Aquifer Region

CMIP5 model ensemble means are shown on the top, and CMIP6 model ensemble means are shown on the bottom, with two corresponding emissions trajectories. The historical monthly precipitation totals are denoted in black in both subfigures.

Future drought projections, introduced in Section **Error! Reference source not found.**, are described and analyzed in this section relative to historical conditions. Section 4.1 presents an analysis of the future temperature and precipitation projections relative to the historical data during noteworthy historic droughts. Historical weather data from the Daymet dataset are used for 1981–2020 to estimate precipitation totals across the Edwards Aquifer Region in Section 4.1.2.1. Historical weather data from the San Antonio International Airport weather station are used for 1947–present to estimate precipitation totals and average temperatures in Section 4.1.2.2. Future CMIP GCM simulations provided by EAA are used for 2021–2060 in both analyses.

4.1 Historical Drought and Drought Projections

4.1.1 Key Takeaways

- To understand how future precipitation could change during periods of drought, gridded and point-based minimum precipitation projections were also developed for drought conditions.
- For the gridded analysis across the Edwards Aquifer region, most models project similar to slightly lower minimum precipitation relative to historical minimum precipitation levels for all drought durations except for the 1- and 7.5-year droughts, which increased for most models.
- For the point-based analysis at the San Antonio International Airport weather station, which includes the 1950s drought of record, nearly all models project increased minimum precipitation relative to historical minimum precipitation levels for all precipitation drought durations.
- Precipitation drought projections tend to be higher under higher emissions scenarios (RCP 8.5, SSP5-8.5) than moderate emissions scenarios (RCP 4.5, SSP2-4.5).
- Within each model drought ensemble, there is a wide range of projected minimum precipitation totals suggesting a high degree of uncertainty in future precipitation.

4.1.2 Results

4.1.2.1 Gridded Edwards Aquifer Region Drought

Table 4 illustrates different historical and model precipitation drought projections averaged across the Edwards Aquifer region. Overall, longer-duration precipitation droughts are projected to experience slight drying through the end of the permit term relative to the past 40 years in the historical record. The ensemble mean projections generally suggest lower precipitation totals for most drought durations, except for 1- and 7.5-year duration precipitation droughts that project an increase in lowest precipitation totals under the model ensemble mean. While most models project drier precipitation totals during the most severe droughts, there is a wide range of projected precipitation totals within each model ensemble, and some models suggest increasing precipitation

totals for all drought durations. This underscores that any changes in future precipitation during the most severe precipitation droughts come with a high degree of uncertainty. It is important to note that as drought duration increases, the range of modeled precipitation decreases, therefore the confidence in decreasing precipitation totals increases. This is likely an artifact of both (1) the loss of year-to-year variability as precipitation is summed over longer-duration events and (2) a reduction in the number of droughts sampled (e.g., more 1-year periods relative to 7.5-year periods during a fixed 2021–2060 future timeframe).

Table 4. Lowest Precipitation Totals under Modeled and Historical Drought Projections averaged across the Edwards Aquifer Authority Region

Drought projections are presented as the lowest precipitation totals (in inches) during consecutive 1-, 2-, 3-, 4-, and 7.5-year periods within each time horizon (1981–2020 for historical, 2021–2060 for future modeled). To demonstrate the full range of potential climate futures, the model ensemble for each emissions scenario and model (CMIP5: RCP 4.5, RCP 8.5; CMIP6: SSP2-4.5, SSP5-8.5) is presented as an ensemble minimum, mean, and maximum.

Drought Scenarios: Precipitation							
Drought Duration	Historical Precipitation (inches)	Historical Drought Dates	Version	Emissions Scenario	Model Ensemble Minimum	Model Ensemble Median	Model Ensemble Maximum
1-year	8.4	2010-09-26 to 2011-09-26	CMIP5	RCP 4.5	7.2	8.1	11.7
				RCP 8.5	7.1	11	16
			CMIP6	SSP2-4.5	6.5	9.0	14
				SSP5-5.8	5.4	9.3	12
2-year	32	2007-09-05 to 2009-09-04	CMIP5	RCP 4.5	24	27	35
				RCP 8.5	22	34	44
			CMIP6	SSP2-4.5	25	29	37
				SSP5-5.8	29	33	36
3-year	65	2010-09-08 to 2013-09-07	CMIP5	RCP 4.5	46	56	70
				RCP 8.5	37	56	72
			CMIP6	SSP2-4.5	50	56	63
				SSP5-5.8	56	58	71
4-year	87	2007-09-14 to 2011-09-14	CMIP5	RCP 4.5	67	86	88
				RCP 8.5	78	85	104
			CMIP6	SSP2-4.5	73	75	89
				SSP5-5.8	77	89	98
7.5-year	184	2007-09-05 to 2015-03-06	CMIP5	RCP 4.5	147	193	202
				RCP 8.5	186	201	222
			CMIP6	SSP2-4.5	162	181	190
				SSP5-5.8	170	189	207

Figure 14 illustrates 2021–2060 modeled precipitation drought projections relative to 1981–2020 observations graphically. Higher emission trajectories (RCP 8.5, SSP5-8.5), shown in red, tend to project higher precipitation totals than moderate emissions trajectories (RCP 4.5, SSP2-4.5), shown in blue. This is likely at least partially due to the projected intensification of the water cycle with warming temperatures.

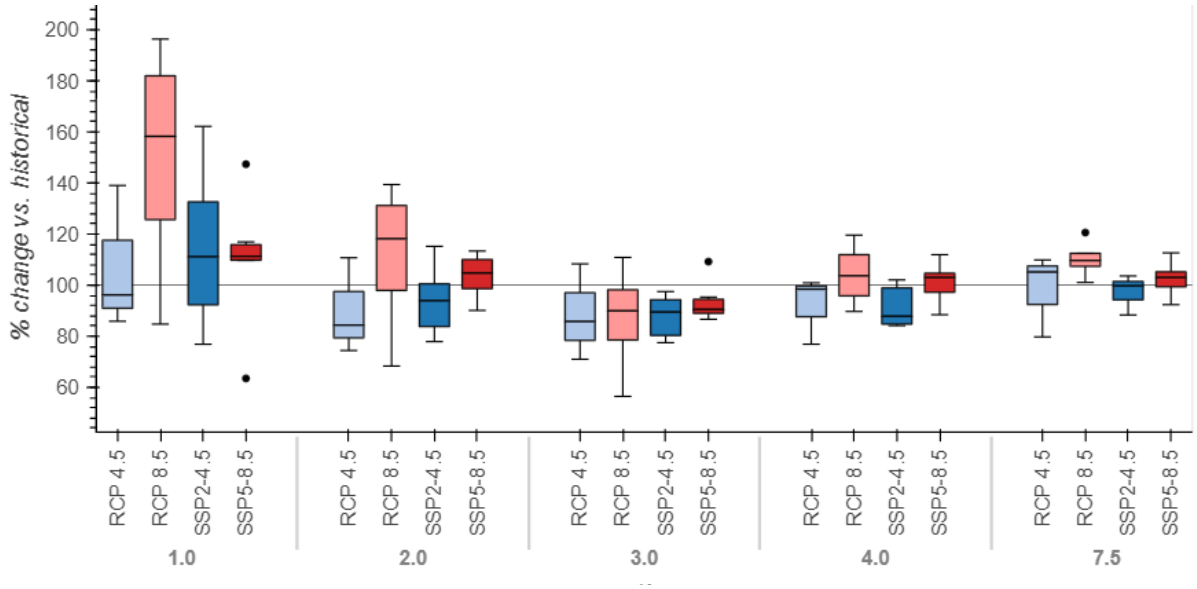

Figure 14. 2021–2060 Modeled Precipitation Drought Projections Relative to 1981–2020 Observations

Drought projections are presented as the lowest precipitation totals during consecutive 1-, 2-, 3-, 4-, and 7.5-year periods relative to the historical values (Historical: 100%). Boxplots display the ensemble minimum, 25th percentile, 50th percentile (median), 75th percentile, and maximum for each emissions scenario.

4.1.2.2 Point-Based San Antonio International Airport Drought

Table 5 and Figure 15 illustrate different historical and modeled precipitation droughts at the San Antonio International Airport. Overall, minimum precipitation is projected to increase during all drought lengths, including the 7.5-year length associated with the drought of record. For example, under the CMIP6 SSP5-8.5 emissions scenario, the 7.5-year drought precipitation total is projected to increase by roughly 29% (from 146 inches under historical conditions to 188 inches under future conditions). This suggests that that the region may not experience a future 7.5-year period with precipitation as low as the drought of record during the proposed permit term.

The precipitation drought projections presented here are designed to represent worst- or near-worst-case droughts (i.e., minimum precipitation values) and may not represent the exact conditions as those observed during notable historical droughts. Specifically, these precipitation drought scenarios do not use idealized projections for each individual drought in response to emissions trajectories (i.e., perfect representation of the same drought under future conditions), but rather provide representations of precipitation droughts of similar length as notable historical droughts.

Table 5. Lowest Precipitation Totals under Historical and Modeled Drought Projections at the San Antonio International Airport

Drought projections are presented as the lowest precipitation totals (in inches) during consecutive 1-, 2-, 3-, 4-, and 7.5-year periods within each time horizon (1947–present for historical, 2021–2060 for future modeled). To demonstrate the full range of potential climate futures, the model ensemble for each emissions scenario and model (CMIP5: RCP 4.5, RCP 8.5; CMIP6: SSP2-4.5, SSP5-8.5) is presented as an ensemble minimum, mean, and maximum.

San Antonio International Airport Drought Projections—Precipitation							
Drought Duration	Historical Precipitation (inches)	Historical Drought Dates	Version	Emissions Scenario	Model Ensemble Minimum	Model Ensemble Median	Model Ensemble Maximum
1-year	8.9	2010-09-08 to 2011-09-08	CMIP5	RCP 4.5	5.4	11	16
				RCP 8.5	9.3	13	18
			CMIP6	SSP2-4.5	7.3	8.6	14
				SSP5-8.5	7.3	9.9	13
2-year	24	2007-09-04 to 2009-09-03	CMIP5	RCP 4.5	28	28	35
				RCP 8.5	24	36	47
			CMIP6	SSP2-4.5	26	29	39
				SSP5-8.5	30	31	35
3-year	45	1953-12-18 to 1956-12-17	CMIP5	RCP 4.5	52	57	71
				RCP 8.5	41	58	80
			CMIP6	SSP2-4.5	53	56	69
				SSP5-8.5	55	60	72
4-year	64	1953-01-16 to 1957-01-16	CMIP5	RCP 4.5	74	90	94
				RCP 8.5	88	89	106
			CMIP6	SSP2-4.5	74	77	97
				SSP5-8.5	81	90	98
7.5-year	146	1949-08-07 to 1957-02-05	CMIP5	RCP 4.5	156	205	206
				RCP 8.5	188	204	229
			CMIP6	SSP2-4.5	159	179	196
				SSP5-8.5	179	188	231

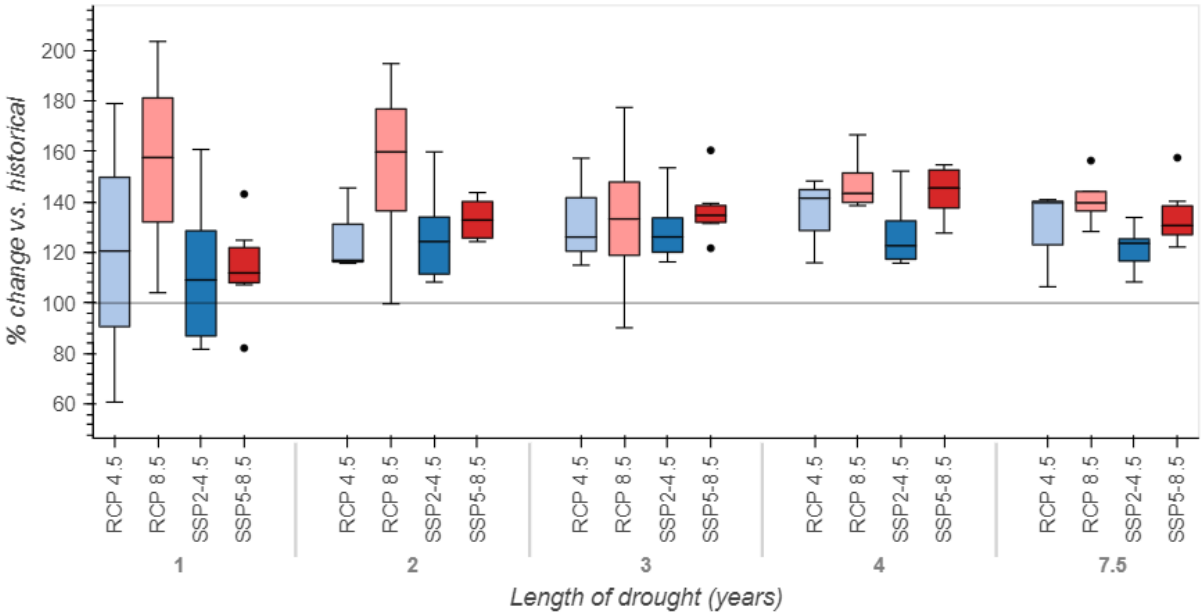

Figure 15. 2021–2060 Modeled Precipitation Drought Projections Relative to 1947-Present Observations

Drought projections are presented as the lowest precipitation totals during consecutive 1-, 2-, 3-, 4-, and 7.5-year periods relative to the historical values (Historical: 100%). Boxplots display the ensemble minimum, 25th percentile, 50th percentile (median), 75th percentile, and maximum for each emissions scenario.

Chapter 5
Discussion

On average, historically the Edwards Aquifer region has experienced drier conditions in the west over the Nueces basin and wetter conditions in the east over portions of the Blanco, Guadalupe, Cibolo, and Med-Cib basins. This has led to a west-to-east, dry-to-wet gradient in annual total precipitation. Historically, temperatures have been warmest in the southern portions of the Edwards Aquifer region. Across the region, while temperatures follow a unimodal seasonal cycle, peaking in late summer, precipitation has historically followed a bimodal seasonal cycle, peaking in late spring and early fall. This renders the region more susceptible to drought conditions during July and August during the warmest months, especially during unusually dry summers.

To inform future modeling efforts and evaluate changes during the proposed permit term, GCM projections of future model-averaged temperature and precipitation were evaluated relative to historical observations. Changes in future GCM-simulated temperature and precipitation may lead to enhanced drought risk across the region in the future, particularly as temperatures warm during anomalously dry periods. Temperatures are projected to increase across all months through 2060, leading to enhanced evapotranspiration rates especially during the warmest summer months.

The region will likely be most susceptible to drought conditions during the warmer late spring to early fall months (May–October). Models project that precipitation will decrease across both emissions trajectories in May, September, and October, while temperature is projected to increase during these months. While precipitation is projected to increase in July and August, it is important to note that these months are projected to experience the largest interannual variability (i.e., year-to-year shifts from high-to-low) in precipitation totals. Unusually dry July and August precipitation totals could lead to enhanced drought conditions by midcentury as temperatures warm.

The largest rates of drying and warming are projected in the western portion of the Edwards Aquifer region in the Nueces basin, which is historically the driest basin in the region. This basin will likely experience the greatest increases in drought risk during the proposed permit term due to decreasing precipitation input and increasing temperatures in a historically dry region.

Last, precipitation drought projections, or worst-case multi-year precipitation deficits (i.e., future minimum precipitation values), were evaluated to understand how noteworthy precipitation droughts may intensify during the permit renewal term. Overall, the region may not experience a future 7.5-year period with precipitation as low as the drought of record during the proposed permit term. Precipitation totals increase for most drought durations in the future relative to the historical period for the 7.5-year drought duration. Analysis of historical and modeled future precipitation at the San Antonio International Airport weather station, in particular, indicates that future minimum precipitation is projected to increase across nearly all model simulations, although precipitation projections come with a high degree of uncertainty.

Chapter 6
References

Başağaoğlu, H., C. Sharma, D. Chakraborty, I. Yoosefdoost, and F.P. Bertetti. 2023. Heuristic data-Inspired Scheme to Characterize Meteorological and Groundwater Droughts in a Semi-Arid Karstic Region under a Warming Climate. *Journal of Hydrology: Regional Studies* 48:101481.

Menne, M.J., I. Durre, B. Korzeniewski, S. McNeill, K. Thomas, X. Yin, S. Anthony, R. Ray, R.S. Vose, B.E. Gleason, and T.G. Houston. 2012: Global Historical Climatology Network - Daily (GHCN-Daily), Version 3.31. NOAA National Climatic Data Center. Available: https://www.ncdc.noaa.gov/cdo-web/search. Accessed: January 2, 2024.

ORNL DAAC. 2020. Daymet. Available: https://daymet.ornl.gov. Accessed: May 17, 2023.

Thornton, M.M., R. Shrestha, Y. Wei, P.E. Thornton, S. Kao, and B.E. Wilson. 2020. Daymet: Daily Surface Weather Data on a 1-Km Grid for North America, Version 4. DAAC, Oak Ridge National Laboratory (ORNL), Oak Ridge, TN. Available: https://daac.ornl.gov/DAYMET/guides/Daymet_Daily_V4.html. Accessed: May 17, 2023.

Wootten, A., H. Başağaoğlu, F.P. Bertetti, L. Schmidt, and D. Chakraborty. 2023. Customized Statistical Downscaling of Gridded Climate Data from Global Climate Models for the Edwards Aquifer Region. Edwards Aquifer Authority, San Antonio, TX.

World Climate Research Programme. 2020. Coupled Model Intercomparison Project (CMIP). https://www.wcrp-climate.org/wgcm-cmip. Accessed: July 22, 2020.

Appendix A
Future Temperature and Precipitation Plots by Basin

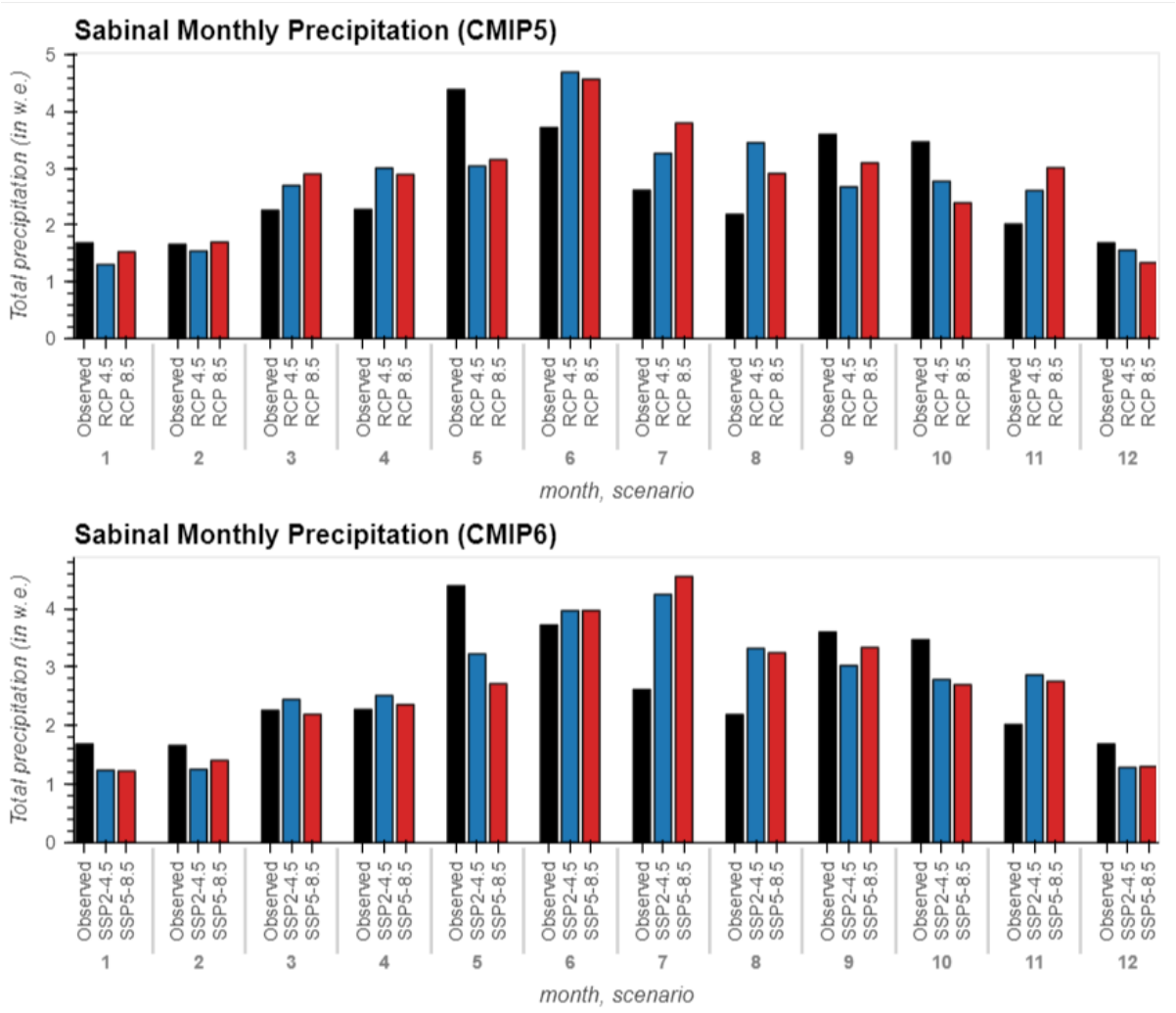

Figure A-1. Mean Monthly Total Precipitation (2030–2059) averaged over the Sabinal Basin

Shown are model ensemble means for CMIP5 (top) and CMIP6 (bottom) and two corresponding emissions trajectories. The historical monthly precipitation totals are denoted in black in both subfigures.

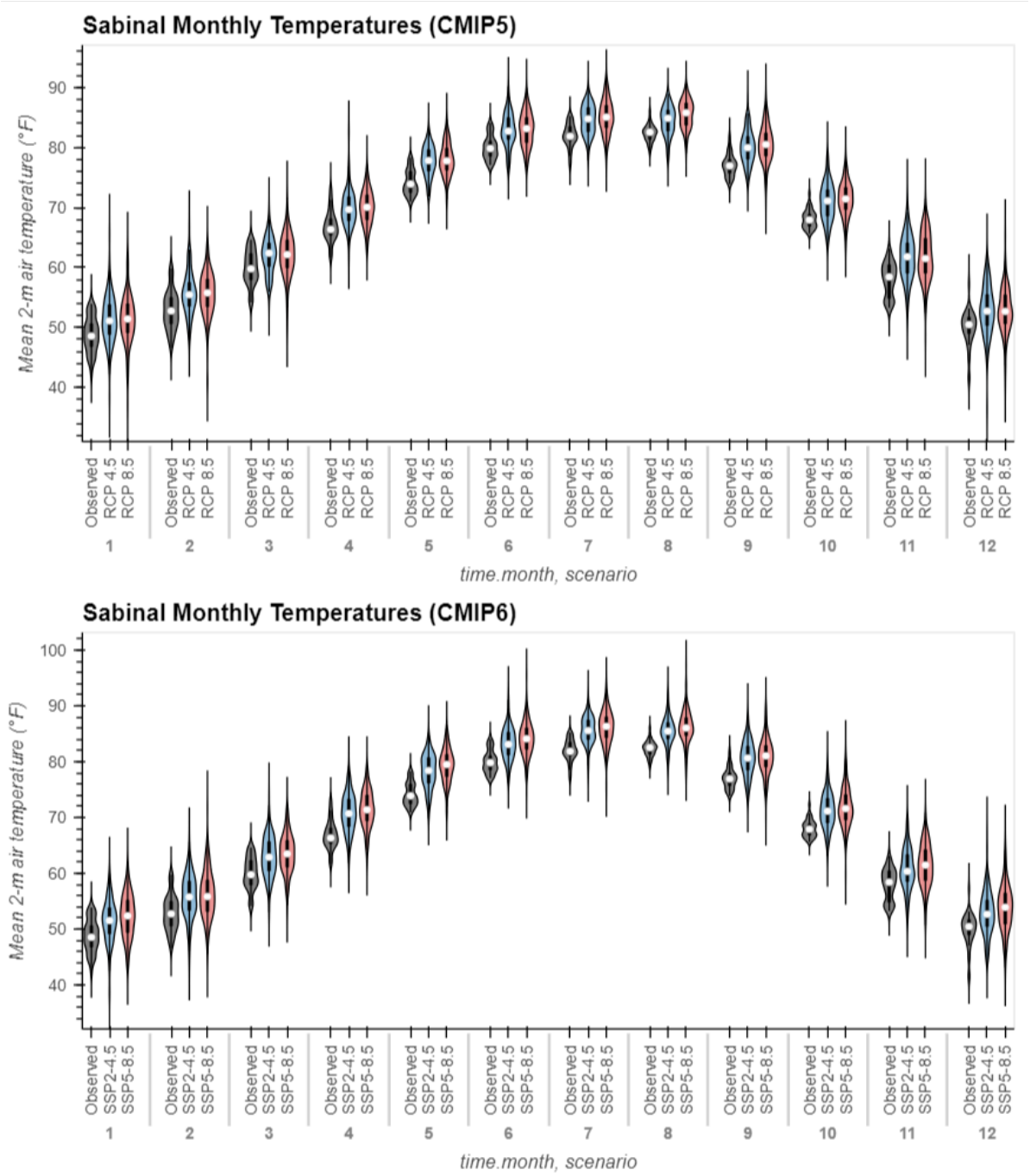

Figure A-2. Violin Plot Distributions of Average Sabinal Basin-Wide Monthly Temperatures (2030–2059)

Shown are CMIP5 (top) and CMIP6 (bottom) model ensembles and two corresponding emissions trajectories. The historical distributions in monthly temperatures (1991–2020) are denoted in black in both subfigures. White dots denote ensemble mean values while black bars represent the 25th–75th interquartile range. Horizontal widths of violin plots represent the density of values (wider = more models with monthly values).

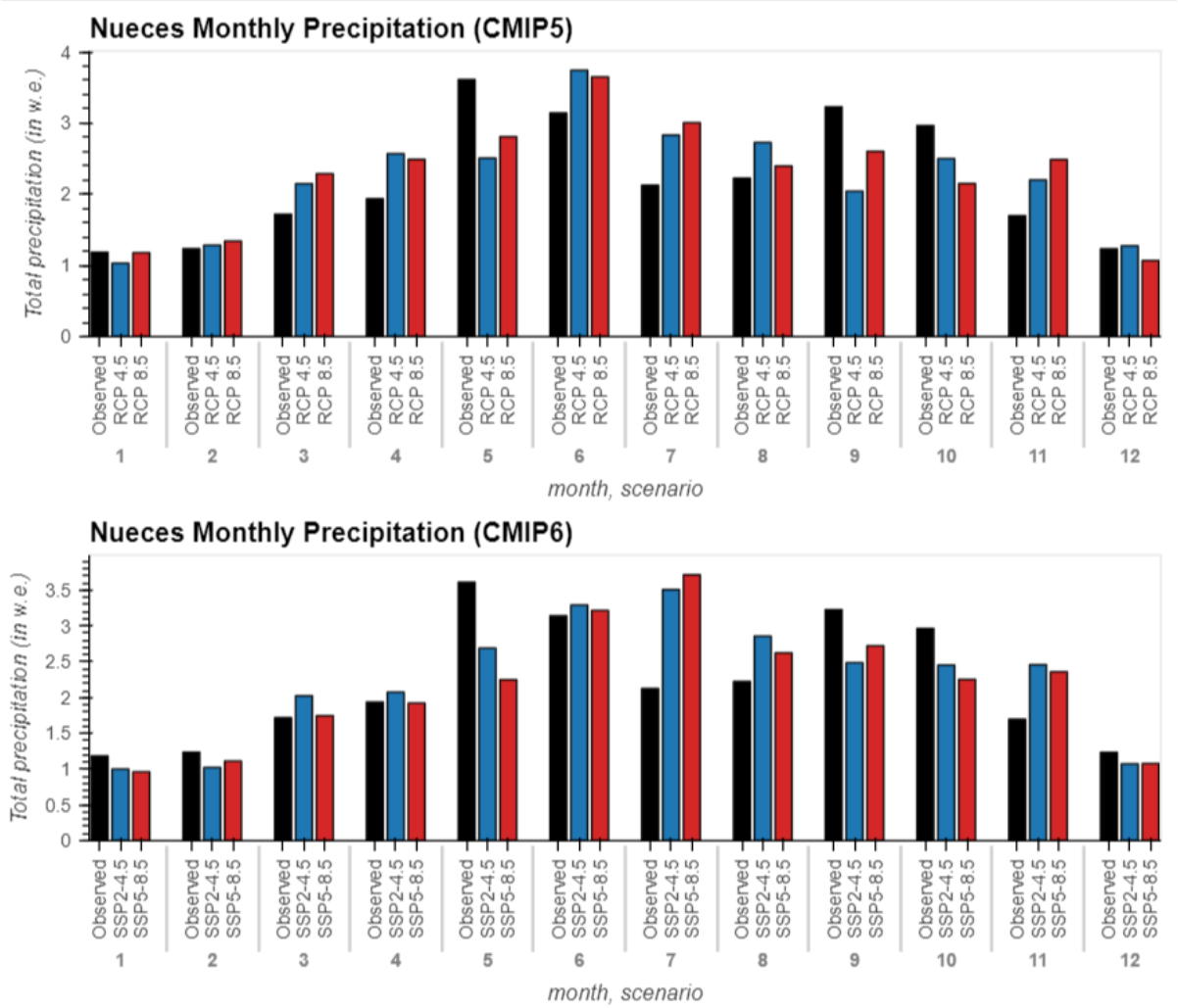

Figure A-3. Mean Monthly Total Precipitation (2030–2059) averaged over the Nueces Basin

Shown are model ensemble means for CMIP5 (top) and CMIP6 (bottom) and two corresponding emissions trajectories. The historical monthly precipitation totals are denoted in black in both subfigures**.**

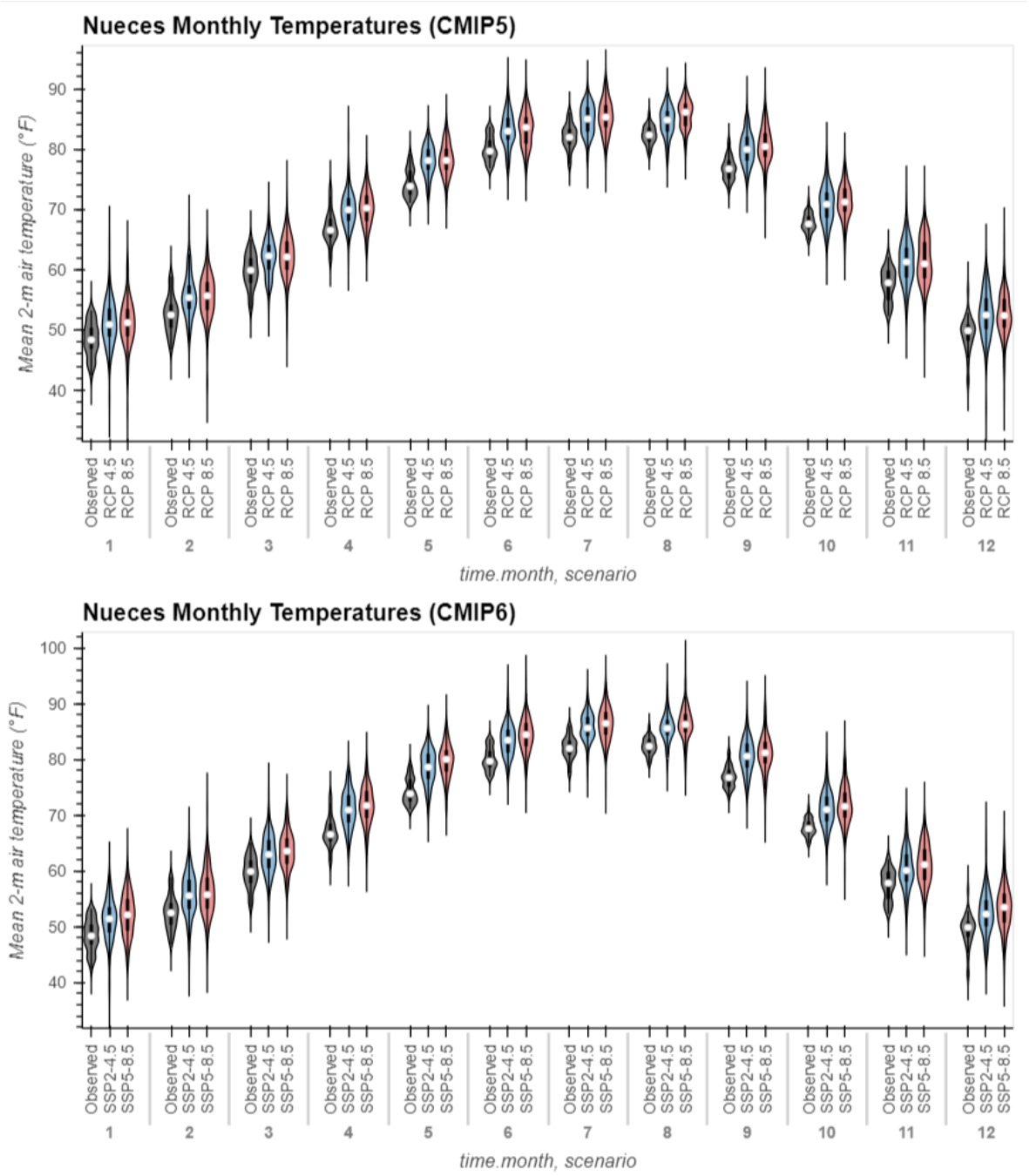

Figure A-4. Violin Plot Distributions of average Nueces Basin-Wide Monthly Temperatures (2030–2059)

Shown are CMIP5 (top) and CMIP6 (bottom) model ensembles and two corresponding emissions trajectories. The historical distributions in monthly temperatures (1991–2020) are denoted in black in both subfigures. White dots denote ensemble mean values while black bars represent the 25th–75th interquartile range. Horizontal widths of violin plots represent the density of values (wider = more models with monthly values).

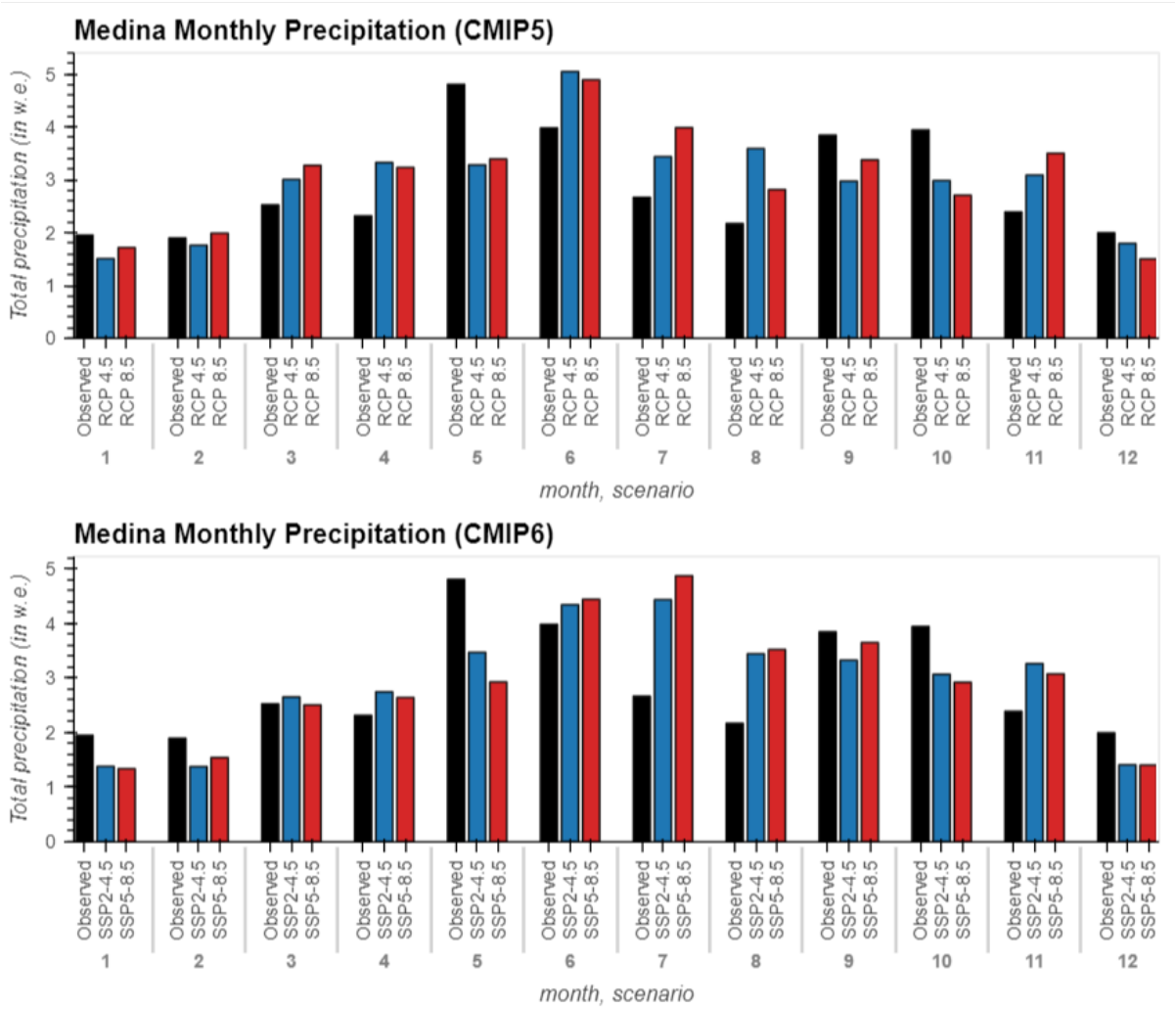

Figure A-5. Mean Monthly Total Precipitation (2030–2059) averaged over the Medina Basin

Shown are model ensemble means for CMIP5 (top) and CMIP6 (bottom) and two corresponding emissions trajectories. The historical monthly precipitation totals are denoted in black in both subfigures.

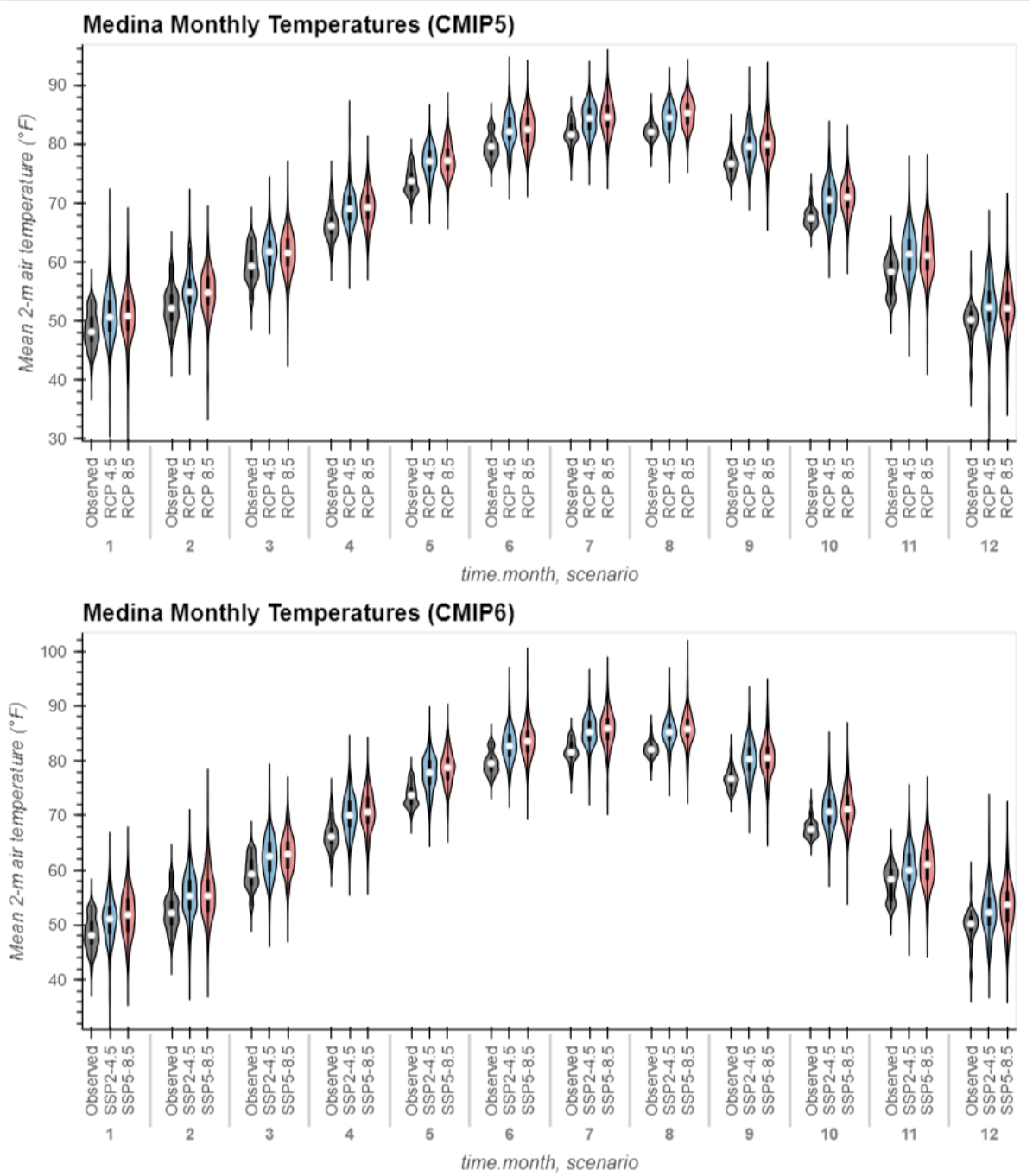

Figure A-6. Violin Plot Distributions of Average Medina Basin-Wide Monthly Temperatures (2030–2059)

Shown are CMIP5 (top) and CMIP6 (bottom) model ensembles and two corresponding emissions trajectories. The historical distributions in monthly temperatures (1991–2020) are denoted in black in both subfigures. White dots denote ensemble mean values while black bars represent the 25th–75th interquartile range. Horizontal widths of violin plots represent the density of values (wider = more models with monthly values).

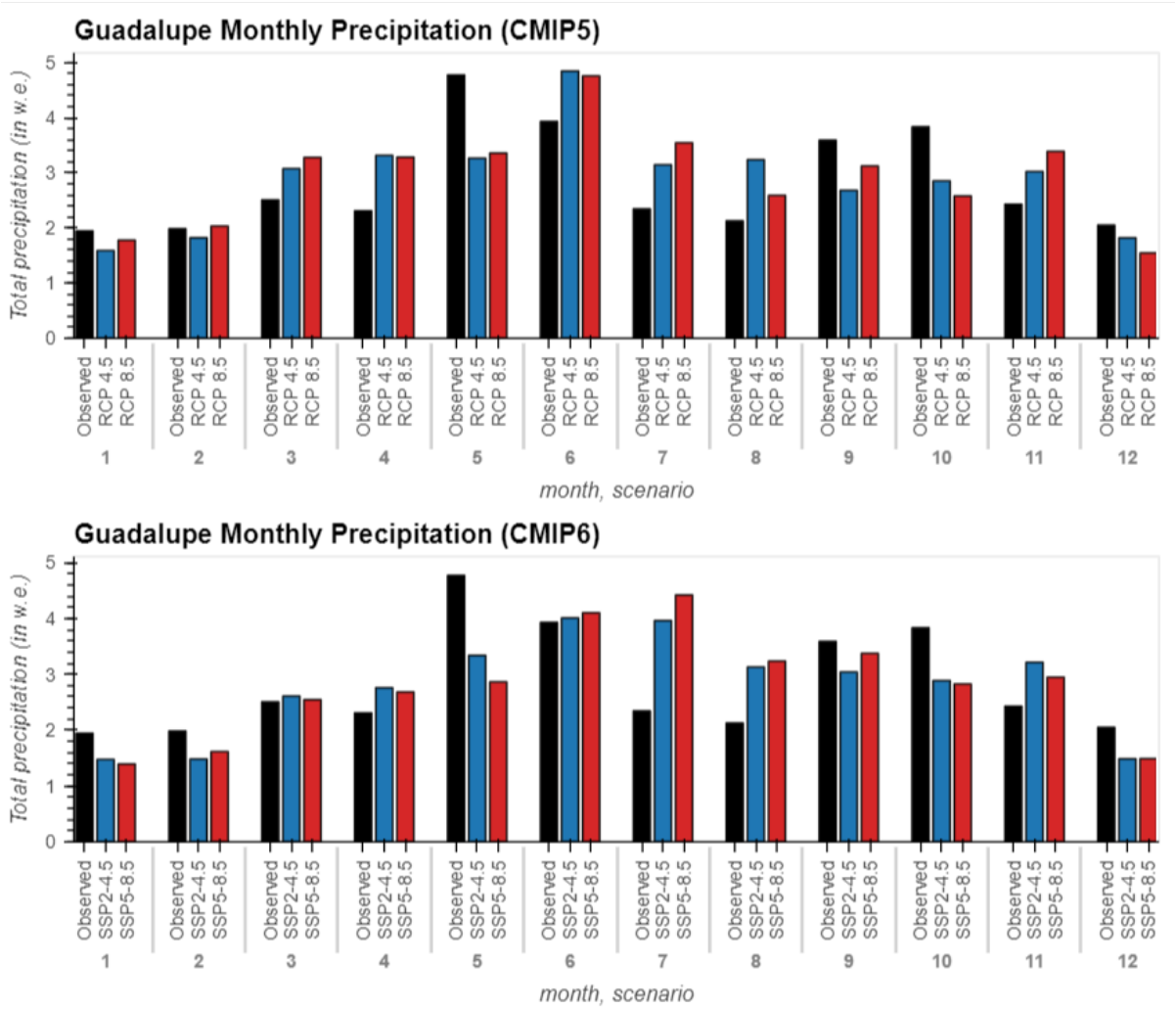

Figure A-7. Mean Monthly Total Precipitation (2030–2059) averaged over the Guadalupe Basin

Shown are model ensemble means for CMIP5 (top) and CMIP6 (bottom) and two corresponding emissions trajectories. The historical monthly precipitation totals are denoted in black in both subfigures.

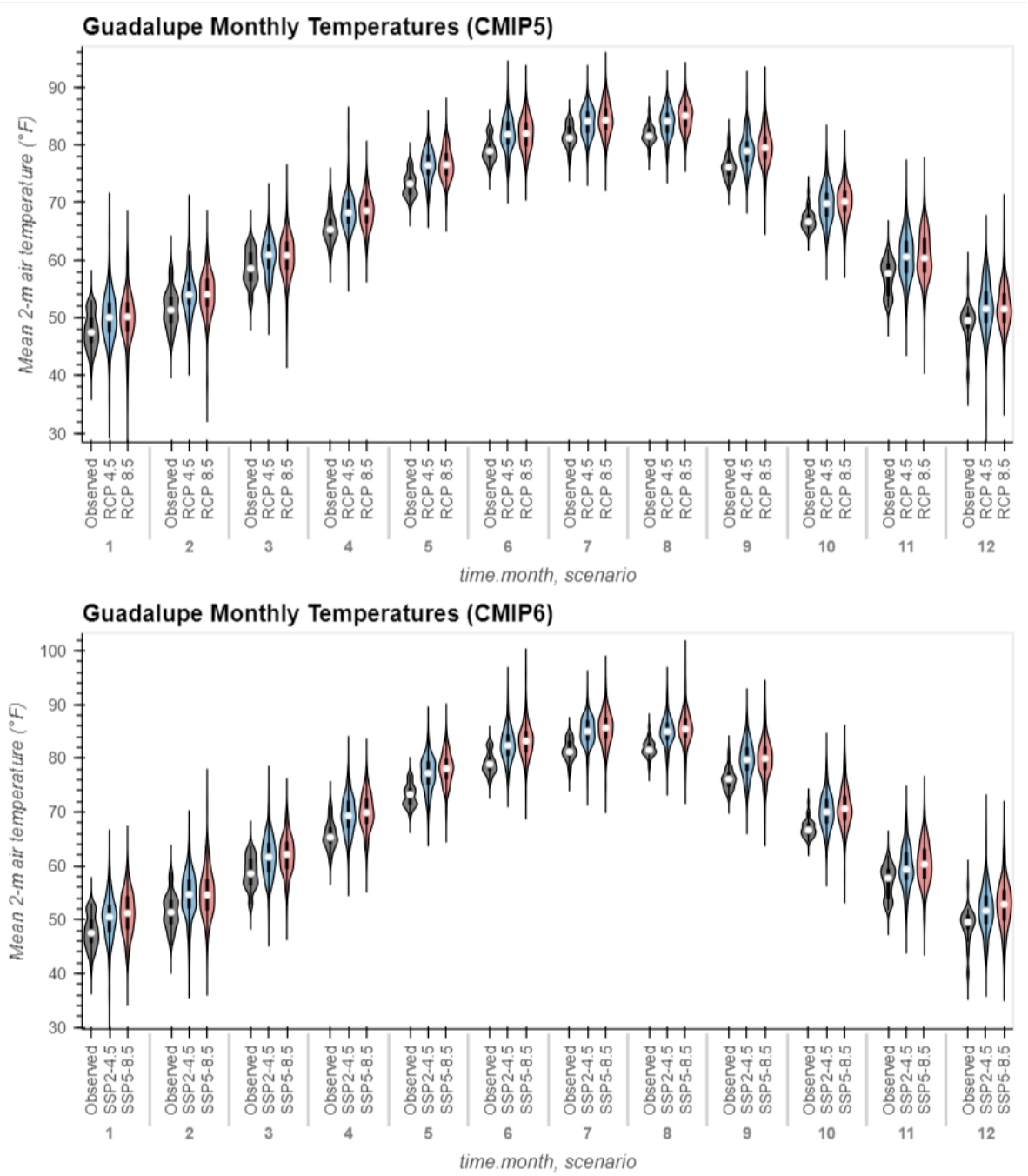

Figure A-8. Violin Plot Distributions of Average Guadalupe Basin-Wide Monthly Temperatures (2030–2059)

Shown are CMIP5 (top) and CMIP6 (bottom) model ensembles and two corresponding emissions trajectories. The historical distributions in monthly temperatures (1991–2020) are denoted in black in both subfigures. White dots denote ensemble mean values while black bars represent the 25th–75th interquartile range. Horizontal widths of violin plots represent the density of values (wider = more models with monthly values).

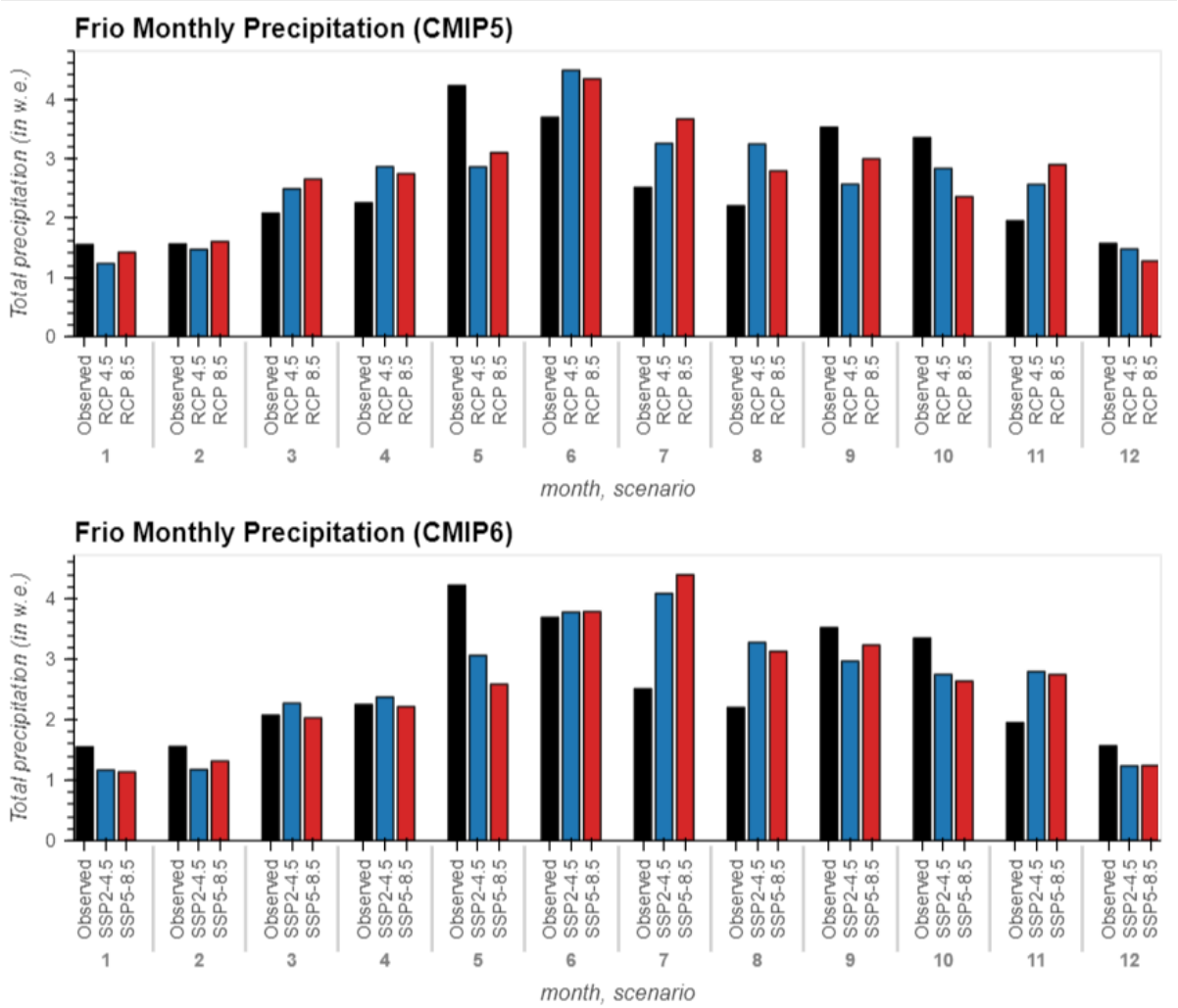

Figure A-9. Mean Monthly Total Precipitation (2030–2059) averaged over the Frio Basin

Shown are model ensemble means for CMIP5 (top) and CMIP6 (bottom) and two corresponding emissions trajectories. The historical monthly precipitation totals are denoted in black in both subfigures.

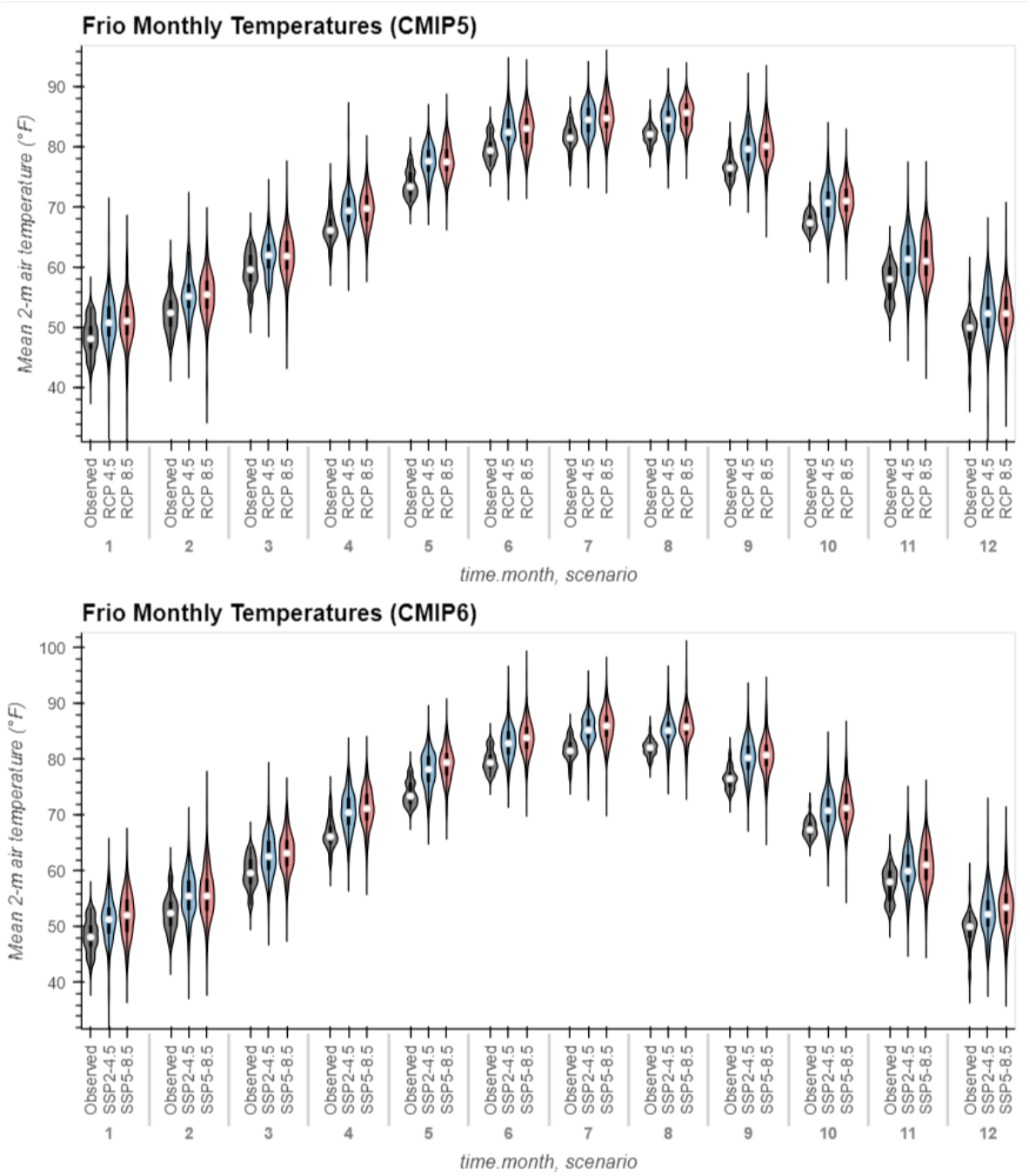

Figure A-10. Violin Plot Distributions of Average Frio Basin-Wide Monthly Temperatures (2030–2059)

Shown are CMIP5 (top) and CMIP6 (bottom) model ensembles and two corresponding emissions trajectories. The historical distributions in monthly temperatures (1991–2020) are denoted in black in both subfigures. White dots denote ensemble mean values while black bars represent the 25th–75th interquartile range. Horizontal widths of violin plots represent the density of values (wider = more models with monthly values).

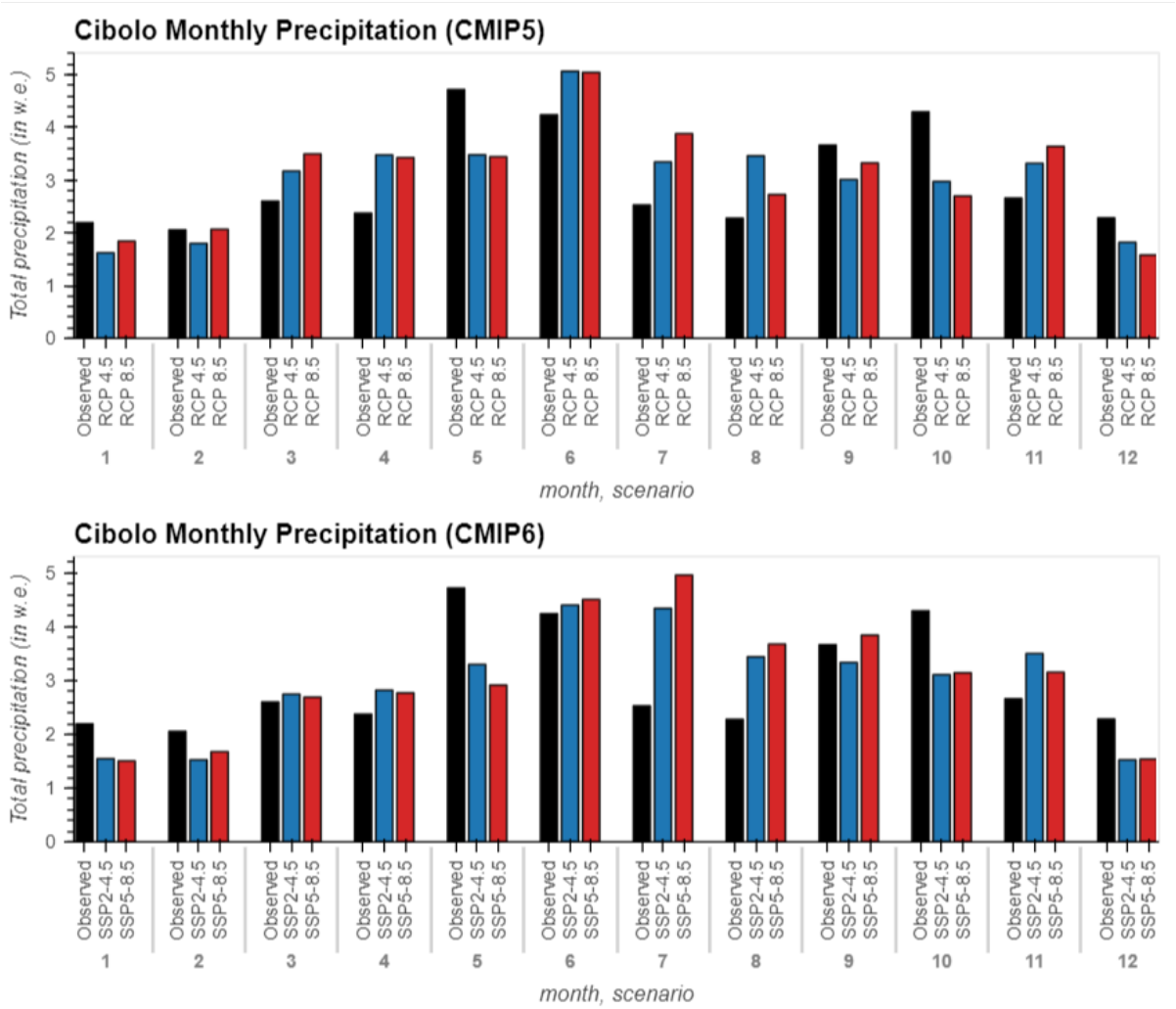

Figure A-11. Mean Monthly Total Precipitation (2030–2059) averaged over the Cibolo Basin

Shown are model ensemble means for CMIP5 (top) and CMIP6 (bottom) and two corresponding emissions trajectories. The historical monthly precipitation totals are denoted in black in both subfigures**.**

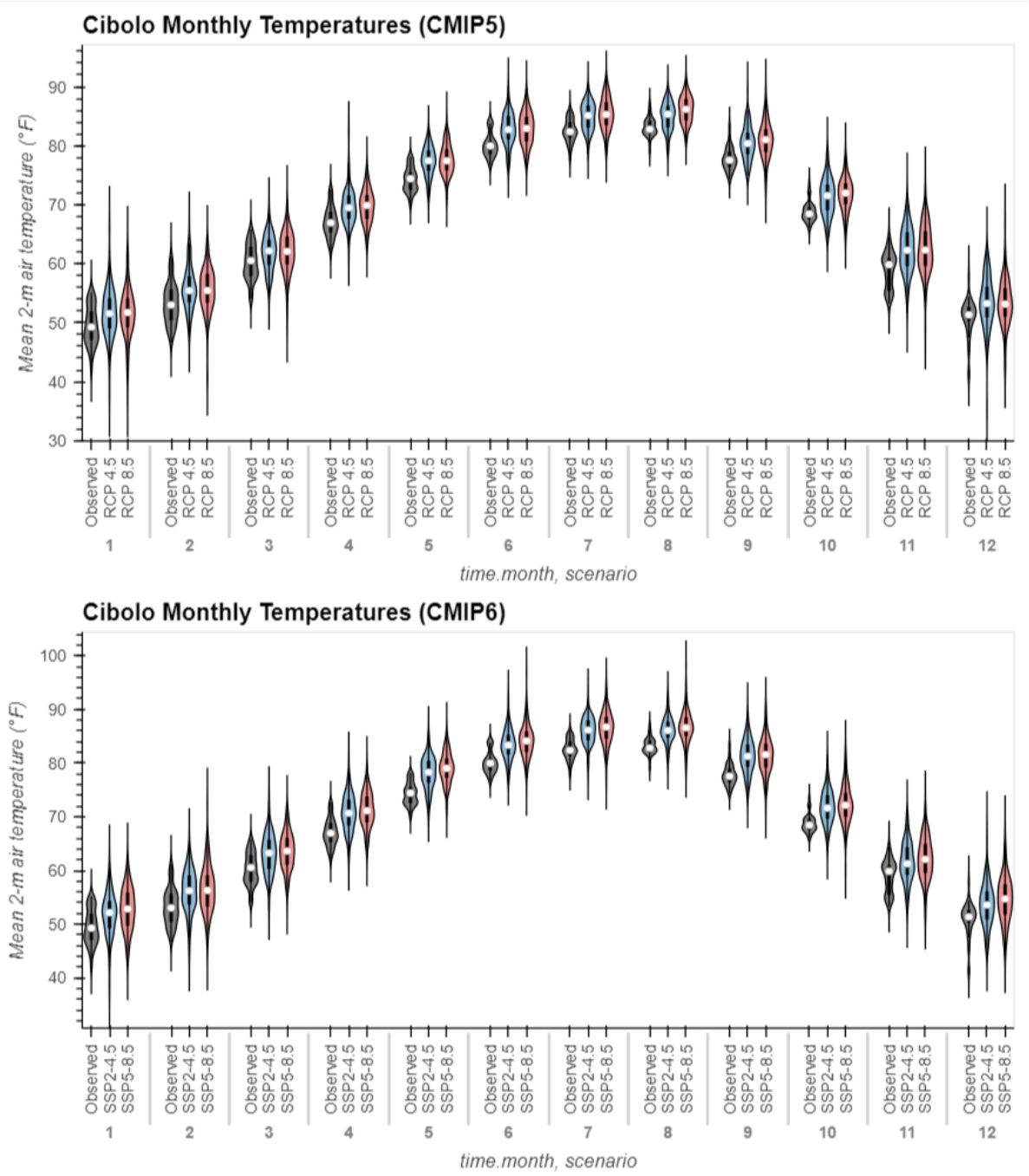

Figure A-12. Violin Plot Distributions of Average Cibolo Basin-Wide Monthly Temperatures (2030–2059)

Shown are CMIP5 (top) and CMIP6 (bottom) model ensembles and two corresponding emissions trajectories. The historical distributions in monthly temperatures (1991–2020) are denoted in black in both subfigures. White dots denote ensemble mean values while black bars represent the 25th–75th interquartile range. Horizontal widths of violin plots represent the density of values (wider = more models with monthly values).

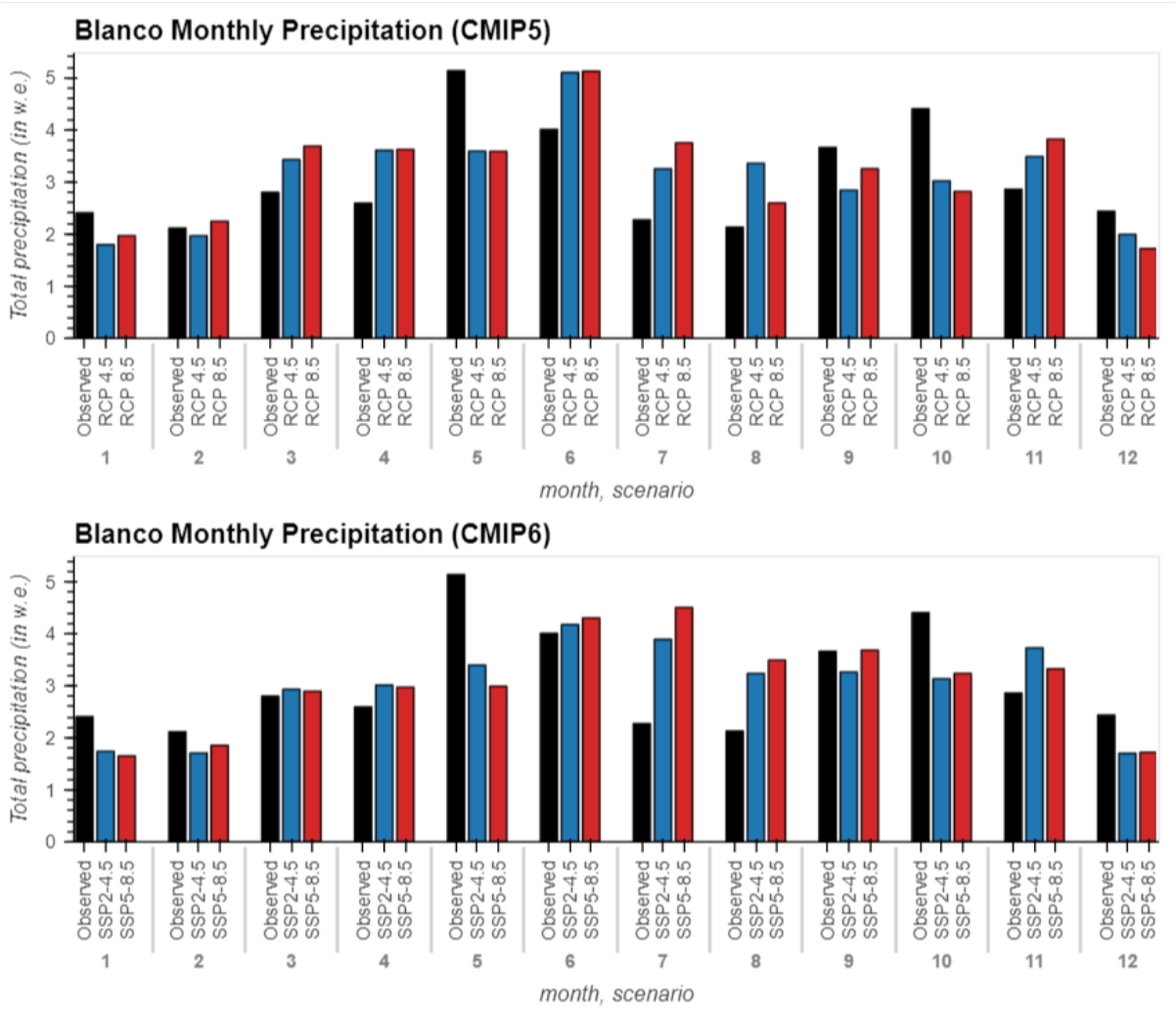

Figure A-13. Mean Monthly Total Precipitation (2030–2059) averaged over the Blanco Basin

Shown are model ensemble means for CMIP5 (top) and CMIP6 (bottom) and two corresponding emissions trajectories. The historical monthly precipitation totals are denoted in black in both subfigures**.**

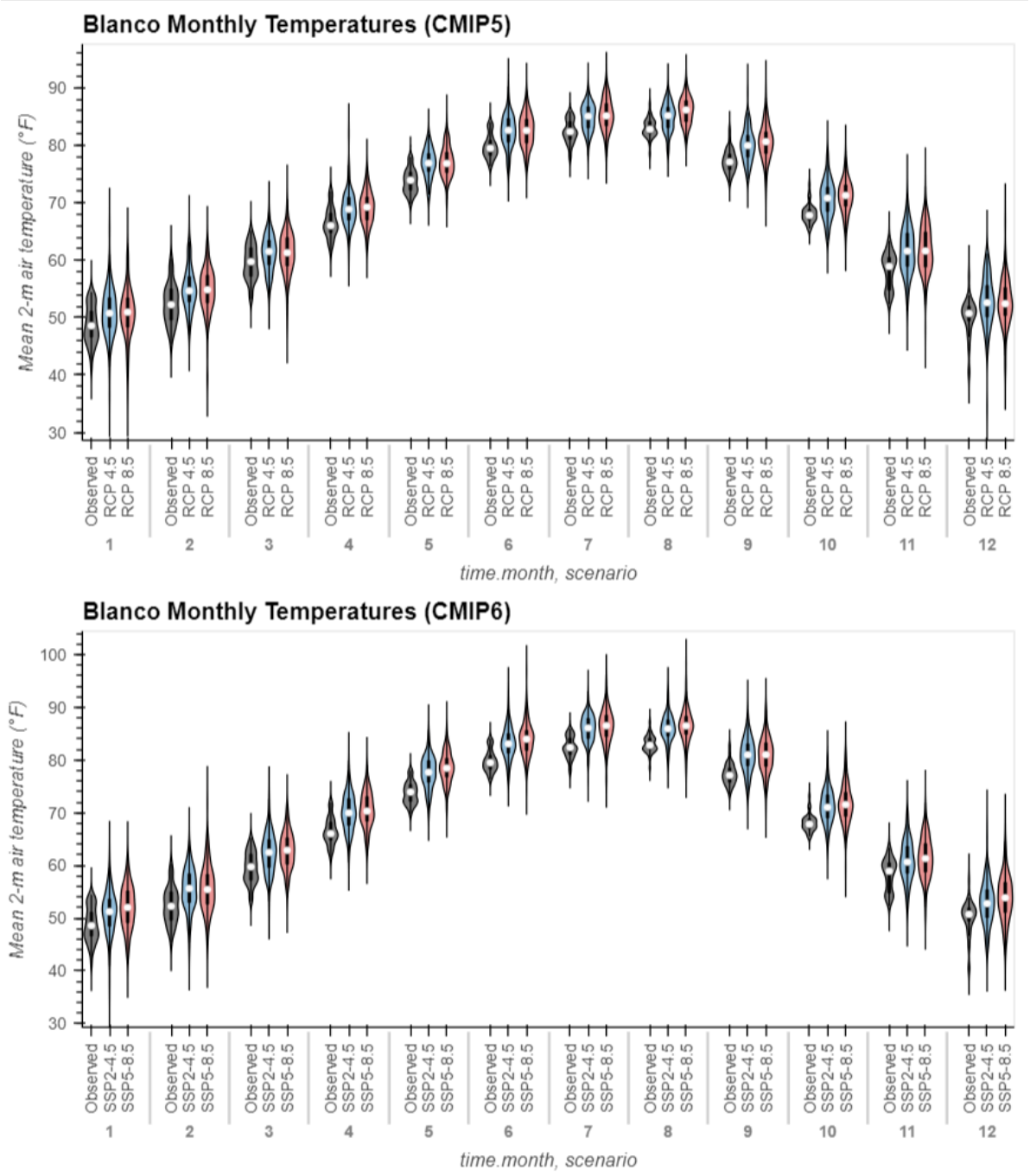

Figure A-14. Violin Plot Distributions of Average Blanco Basin-Wide Monthly Temperatures (2030–2059)

Shown are CMIP5 (top) and CMIP6 (bottom) model ensembles and two corresponding emissions trajectories. The historical distributions in monthly temperatures (1991–2020) are denoted in black in both subfigures. White dots denote ensemble mean values while black bars represent the 25th–75th interquartile range. Horizontal widths of violin plots represent the density of values (wider = more models with monthly values).

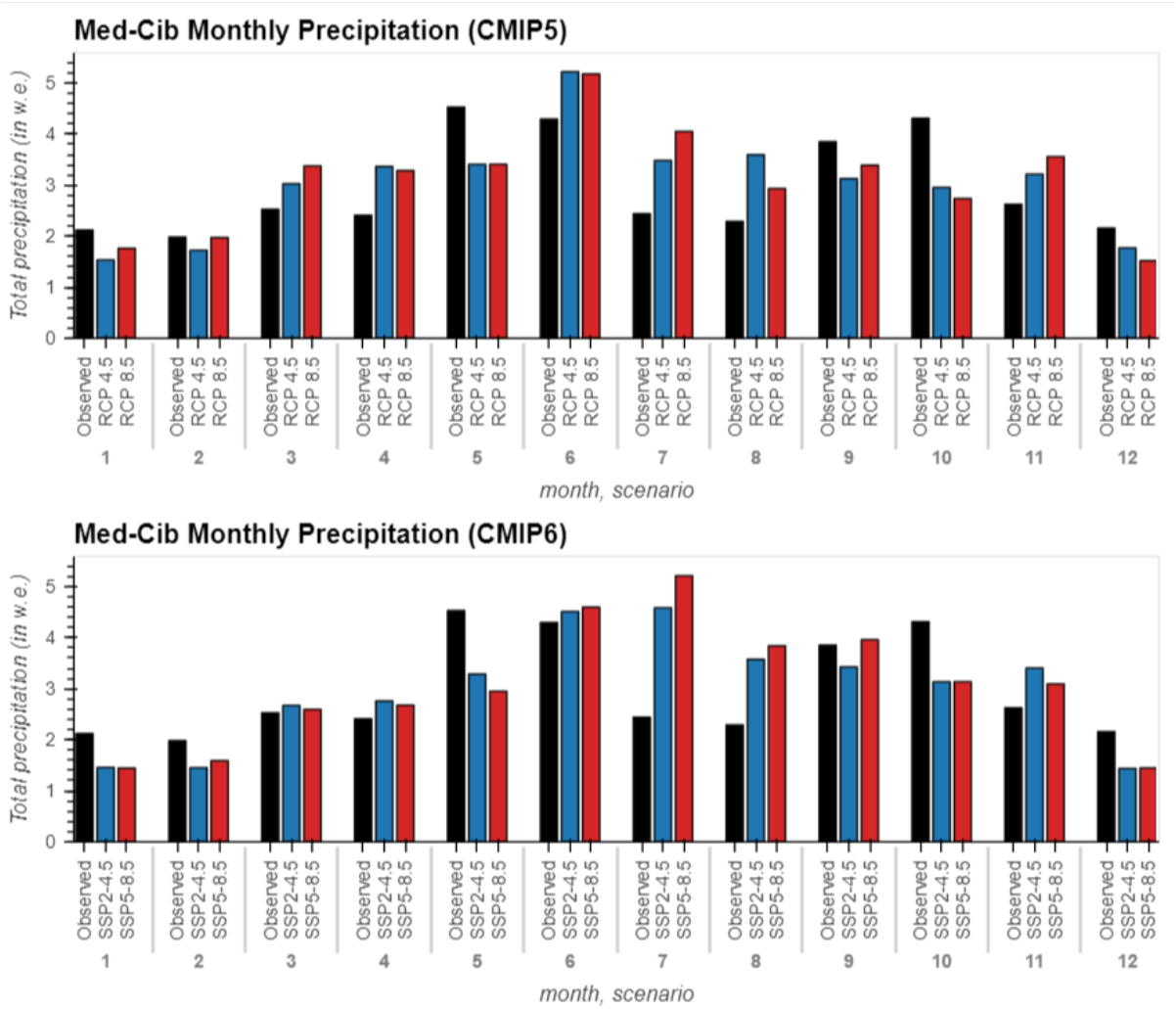

Figure A-15. Mean Monthly Total Precipitation (2030–2059) averaged over the Med-Cib Basin

Shown are model ensemble means for CMIP5 (top) and CMIP6 (bottom) and two corresponding emissions trajectories. The historical monthly precipitation totals are denoted in black in both subfigures**.**

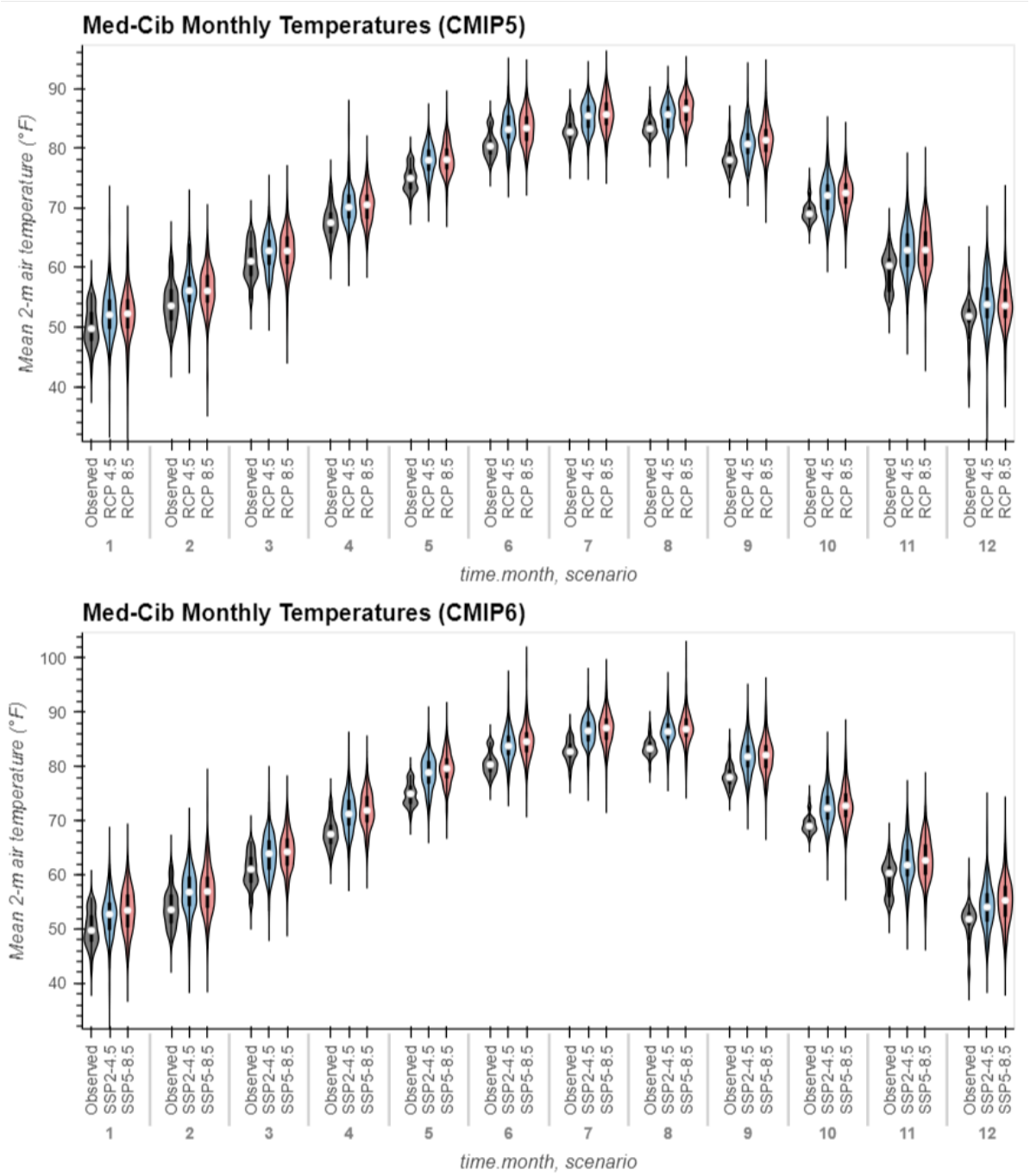

Figure A-16. Violin plot distributions of average Med-Cib basin-wide monthly temperatures (2030–2059)

Shown are CMIP5 (top) and CMIP6 (bottom) model ensembles and two corresponding emissions trajectories. The historical distributions in monthly temperatures (1991–2020) are denoted in black in both subfigures. White dots denote ensemble mean values while black bars represent the 25th–75th interquartile range. Horizontal widths of violin plots represent the density of values (wider = more models with monthly values).

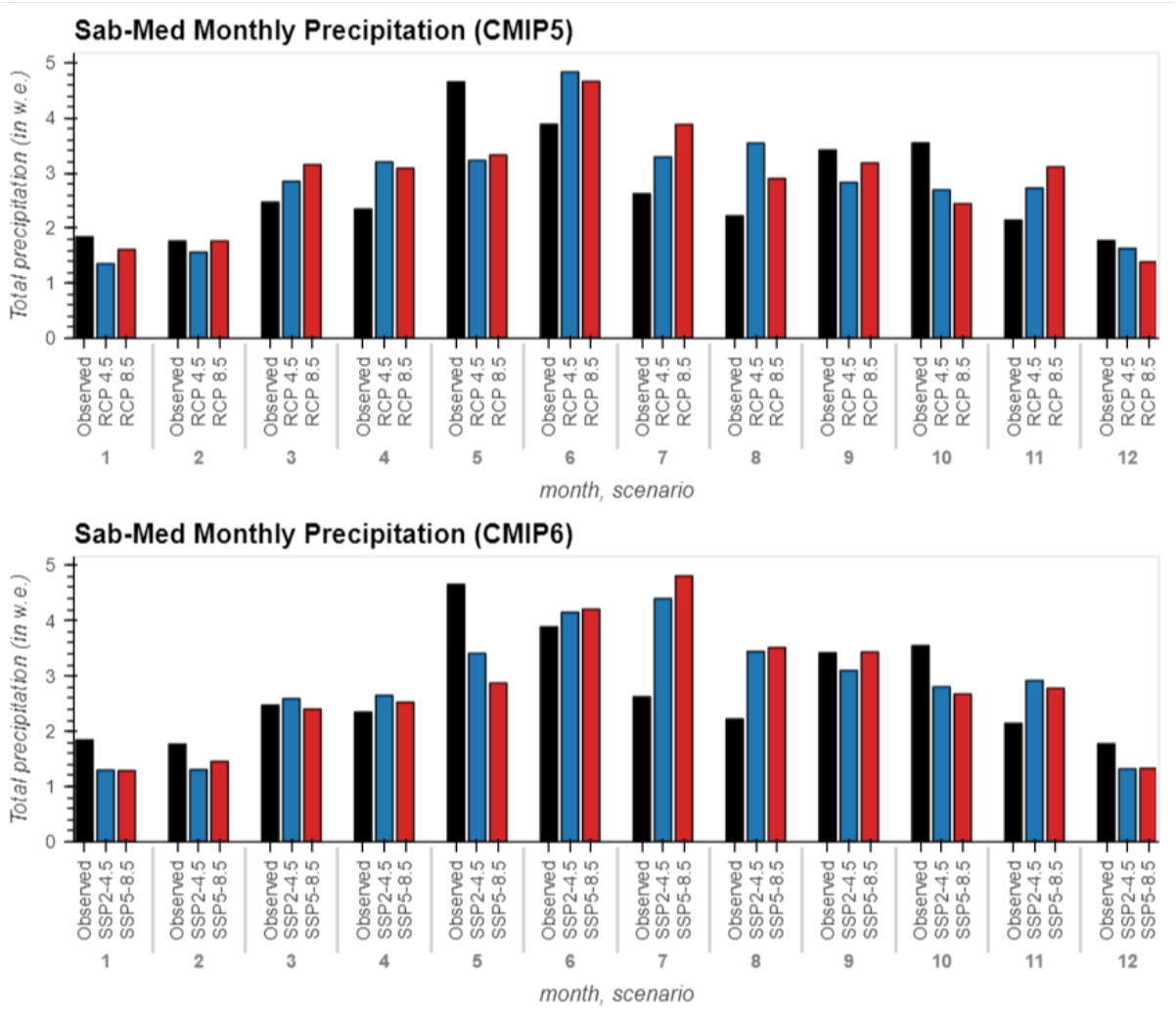

Figure A-17. Mean Monthly Total Precipitation (2030–2059) averaged over the Sab-Med Basin

Shown are model ensemble means for CMIP5 (top) and CMIP6 (bottom) and two corresponding emissions trajectories. The historical monthly precipitation totals are denoted in black in both subfigures**.**

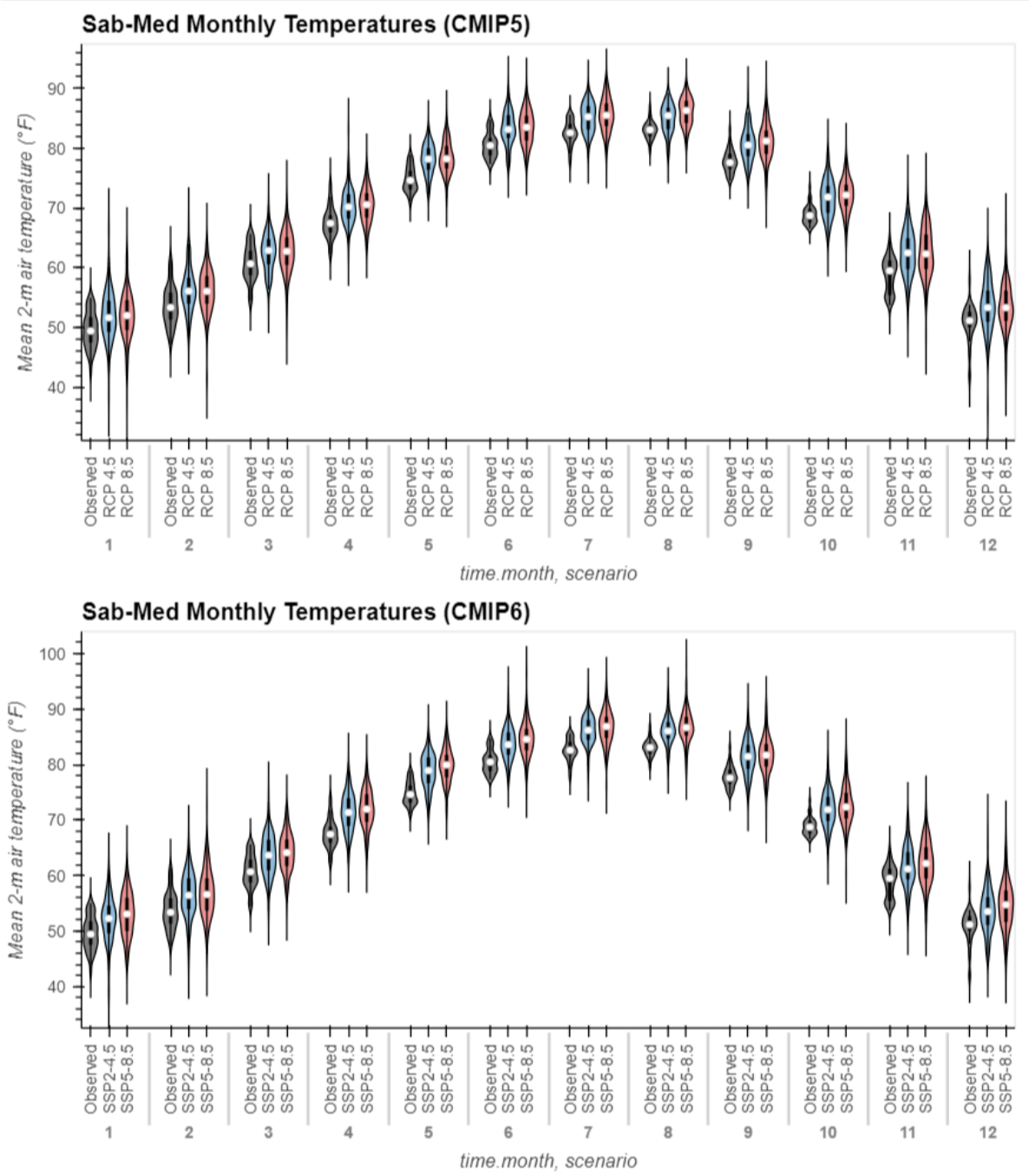

Figure A-18. Violin Plot Distributions of Average Sabinal Basin-Wide Monthly Temperatures (2030–2059)

Shown are CMIP5 (top) and CMIP6 (bottom) model ensembles and two corresponding emissions trajectories. The historical distributions in monthly temperatures (1991–2020) are denoted in black in both subfigures. White dots denote ensemble mean values while black bars represent the 25th–75th interquartile range. Horizontal widths of violin plots represent the density of values (wider = more models with monthly values).

[i] The drought of record occurred from 1951 through 1956 and is characterized by an average recharge for any 7-year period of equal to 168,700 acre-feet as derived for the period 1950–1956.